Thermal conductivity of polymers

C. L. Choy
Department of Physics, The Chinese University of Hong Kong, Hong Kong
(Received 29 April 1976; revised 29 March 1977)

In this review we have concentrated on the interpretation of three essential aspects of the thermal conductivity K of polymers: the temperature dependence, the crystallinity dependence and the orientation effect. K for all amorphous polymers is approximately equal in magnitude and characterized by a T^2 dependence below 0.5K, a plateau region between 5 and 15K and a slow increase at yet higher temperatures. While a number of models involving different phonon scattering mechanisms are capable of explaining these features, further corroborating evidence would be needed to explain the *ad hoc* assumptions involved. For semicrystalline polymers K shows both strong crystallinity and temperature dependence, with a distinctive cross-over point at about 10K. These marked features can now be understood as the result of the interplay between two competing factors: the intrinsically higher conductivity in the crystalline regions, and the reduction in K due to an additional phonon scattering mechanism which becomes important at low temperature. This scattering could arise from either the correlation in the spatial fluctuation of the sound velocity in the polymer or the acoustic mismatch at the interfaces between the crystallites and the amorphous matrix.

Orientation produces a very large anisotropy in semicrystalline polymers, which however decreases at low temperature and becomes insignificant below 10K. This feature can again be understood in terms of the same competing mechanisms if one realizes that the molecular chains in the crystallites are essentially lined up along the direction of orientation thus offering very little thermal resistance along this direction. For polyethylene with an extrusion ratio of 25 the thermal conductivity at 100K along the extrusion direction is 91 mW/cm K, a value extremely high for polymers and close to that of stainless steel. At this temperature the anisotropy is only about 20, yet because of the different temperature dependence of the thermal conductivity along and perpendicular to the extrusion direction, we predict an anisotropy as high as 60 at room temperature.

INTRODUCTION

There have been comparatively few studies of the thermal conductivity of polymers even though this property is of considerable scientific and technological interest. Most of these studies[1] are confined to the range around room temperature and this severely limits our understanding of the different mechanisms which contribute to heat conduction in polymers. Fortunately, this situation has somewhat improved in the past few years and data are now available for a number of polymers in the wider temperature range of 1 to 350K[2–8]. This review attempts to give an interpretation of the effect of temperature, crystallinity and orientation on the thermal conductivity of polymers and to indicate areas in which further investigations are needed for clarifying the situation. In this discussion we will include all the polymers for which data are available over a wide temperature range (1 to 350K). In addition, we will also consider most of the available low-temperature data (1 to 20K) since these have not received sufficient attention in previous reviews[1,9].

Recent studies on a large number of amorphous solids have firmly established the fact that the thermal conductivity (K) of all amorphous solids, whether organic or inorganic, has similar temperature dependence[2–14]. Below 0.5K, K is approximately proportional to T^2; as the temperature rises K increases more slowly until, between 5 and 15K, it becomes independent of T (plateau region). At higher temperatures K again increases until, above 60K, it becomes proportional to the specific heat. Two approaches have been suggested to account for this universal temperature dependence. The first approach[15,16] assumes that the scattering of phonons is due to the spatial fluctuations in the elastic properties of the solid. In the recent formulation by Morgan and Smith[16] the T^2 dependence follows from the assumption of a long correlation length for these fluctuations of the order of 3000 Å, while the plateau is explained by the increasing importance, with rising temperature, of a short-range correlation of the order of 10 Å. In the second approach[17,18] resonant scattering by tunnelling states is assumed to be the dominant scattering mechanism for phonons at very low temperatures and this leads to the T^2 dependence. Furthermore, the plateau region can be explained by scattering by a different band of localized states at higher frequencies[19]. However, very little is known about the nature of these tunnelling or localized states except that there is some evidence of their existence in the data of specific heat and ultrasonic absorption. At the moment, both approaches seem to give an equally plausible explanation for the temperature dependence of amorphous materials and they will be discussed in detail in the following sections.

The temperature dependence of K of semicrystalline polymers is vastly different from that of the amorphous ones[2–8, 20–24]. The plateau region is absent and K normally exhibits a T^1 to T^3 dependence between 0.1 and 20K. At higher temperatures, K increases more slowly up to their respective glass transition temperatures, except for the highly crystalline polymers such as polyethylene (PE) and polyoxymethylene (POM), for which K reaches a peak near 100K and then decreases slowly with temperature. K also depends strongly on the degree of crystallinity and this is exemplified by the case of poly(ethylene terephthalate) (PET)[7,24]. While

K of PET at 30K and above increases with increasing crystallinity, the values below about 10K show the opposite trend. At 1.5K, K of a 50% crystalline sample is one order of magnitude lower than that of the amorphous material.

This unusual behaviour has been explained by considering a semicrystalline polymer as a composite consisting of crystalline lamellae embedded in an amorphous matrix. Then the increase of K with crystallinity at high temperature can be understood as the reflection of the higher average conductivity of the crystalline regions. However, the cross-over of the conductivity and the subsequent large decrease for the semicrystalline samples reveal an additional scattering mechanism which becomes important at low temperatures. This strong scattering process has been treated in two separate approaches which are valid in different temperature range (i.e. different phonon wavelength range). In the first treatment the presence of crystallites is assumed to introduce an additional correlation length ($\simeq$ 100 Å) for the fluctuation of the sound velocity and the increase in phonon scattering (with the accompanying decrease in conductivity) can be calculated either using the Klemens[15,24] or the Morgan–Smith models[6,16]. It has been emphasized[16] that this approach works only when the phonon mean free path is larger than the correlation length, and this condition holds below about 5K. The second model[7] assumes that the difference in elastic properties between the amorphous and crystalline regions gives rise to a thermal boundary resistance R_b at the interface. Direct measurements[25–27] of R_b for a number of solids show that it increases with decreasing temperature and becomes proportional to T^{-n} $(2 < n < 2.7)$ below 4K, which is in slight disagreement with Little's[28] theoretical prediction of T^{-3}. Nevertheless, this rapid increase in R_b can certainly account for the much smaller conductivity of the semicrystalline samples[7]. Although there is no simple criterion for the validity of this treatment it certainly will not be valid below 2K where the dominant phonon wavelength is larger than both the crystallite size and the distance between crystallites.

The last topic to be covered in this article is the effect of orientation on the thermal conductivity of semicrystalline polymers. Contrary to the case for amorphous polymers where orientation effect above 100K has been investigated in some detail[1,29–32], work on semicrystalline polymers has been reported only recently[8,33–36]. On comparing these data, it is clear that semicrystalline polymers show a much larger anisotropy, but this effect diminishes with decreasing temperature and becomes insignificant below 10K. For instance, whereas at 100K a high density polyethylene sample extruded to 13 times its original length has a thermal conductivity in the extrusion direction ($K_\parallel$) equal to 10 times the value in the perpendicular direction ($K_\perp$), the corresponding ratio below 10K is only about 1.5[34].

These contrasting effects can also be explained by the composite model in the following manner. When a semicrystalline polymer is oriented, the spherulitic structure is deformed and gradually broken up. Even at low extrusion ratios such as 4, the chain axes (c-axes) within the crystalline lamellae are mostly aligned along the extrusion direction. Since the covalent bonds along the chains are much stronger than the van der Waals bonds across the chains, the thermal resistance along the c-axis of a crystallite is negligible compared to that in the perpendicular direction. Thus the crystalline regions in an oriented sample provide almost no resistance to heat flow along the extrusion direction, and so at high temperatures, $K_\parallel$ will be much larger than $K_\perp$. However, at low temperatures, the dominant resistive mechanism (either arising from correlation in sound velocity fluctuation or boundary resistance) is not expected to be much affected by the orientation of the chains in the crystalline regions so the orientation effect is much smaller. We will see how these ideas can be applied to interpret the data of a few oriented semicrystalline polymers.

AMORPHOUS POLYMERS

General considerations

In insulating solids heat conduction takes place by means of the lattice vibrations. Theoretical effort has been mainly confined to crystalline solids where the lattice vibrations can be resolved into normal modes which can then be quantized giving rise to the concept of phonons. These phonons are particles obeying Bose–Einstein statistics and the heat current is determined by the phonon distribution which can be obtained by solving the Boltzmann equation. The thermal conductivity is then given by[37]:

$$K(T) = \frac{1}{3}\sum_i \int C_i(\omega) v_i l_i(\omega) \mathrm{d}\omega \qquad (1)$$

where $C_i(\omega)\mathrm{d}\omega$ is the heat capacity contribution of phonons of polarization i and frequency ω, v_i is the phonon velocity and $l_i(\omega)$ is the phonon mean free path. In the Debye approximation where $C_i(\omega)$ is a known function and v_i is independent of ω, $K(T)$ is determined by $l(\omega)$. Thus the whole problem reduces to the calculation of the phonon mean free path $l(\omega)$.

Equation (1) can be considerably simplified by using the dominant phonon approximation. This follows from the fact that, at any temperature T, the phonons which contribute significantly to the integral in equation (1) have frequency $\omega \simeq 4kT/\hbar$. Thus the frequency dependence of l can be converted to an equivalent temperature dependence and, after averaging over all polarizations, equation (1) becomes:

$$K(T) = \frac{1}{3} C(T) v l(T) \qquad (2)$$

where C is the heat capacity per unit volume and v is the average phonon velocity. This is exactly the expression obtained if the kinetic theory of gases is applied to a system of phonons. At sufficiently low temperatures where $C \propto T^3$, a frequency dependence of $l \propto \omega^{-n}$ will result in $K \propto T^3 T^{-n} = T^{3-n}$. Therefore the temperature dependence of K will provide vital information on the dominant scattering mechanism at low temperatures.

The temperature dependence of the thermal conductivity of crystalline solids (see α-quartz in *Figure 1*) can be understood qualitatively by means of equation (2). At high temperatures where most of the phonons are excited, the probability of interaction among the phonons through the Umklapp processes[37] is proportional to the number of phonons, i.e. to the temperature. Thus l is proportional to T^{-1} and since $C \simeq$ constant it follows that $K \propto T^{-1}$. As the temperature is reduced fewer phonons are available for interaction and this leads to an exponential increase in both l and K. For crystalline solids containing defects or impurities this exponential rise is usually not observed but the net effect is still a rapid

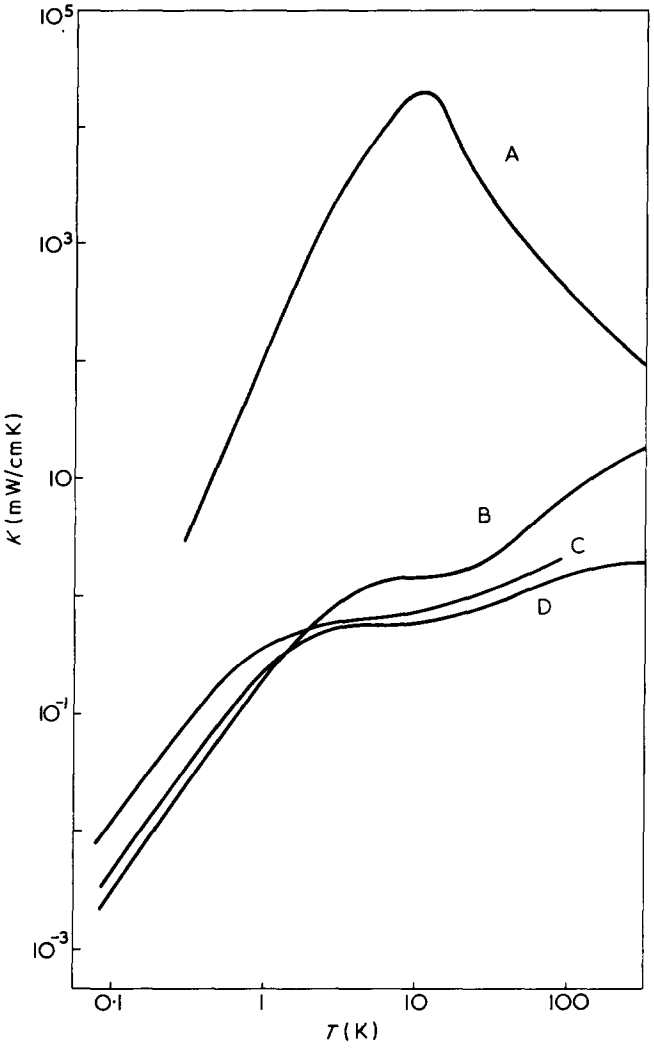

Figure 1 Thermal conductivity of crystalline and amorphous SiO_2, amorphous selenium (Se) and poly(methyl methacrylate) (PMMA). The data for SiO_2 and Se after Zeller and Pohl (ref 14); data for PMMA from refs 3, 5, 11 and 12. A, α-quartz, // c-axis; B, vitreous silica; C, Se; D, PMMA

increase in l until its value reaches the dimension of the sample. The phonons will then be scattered by the boundaries of the sample giving rise to a constant mean free path. Thus the thermal conductivity passes through a maximum and then becomes proportional to the specific heat, i.e. to T^3 at low temperatures.

Figure 1 also shows the thermal conductivity of a few amorphous solids. It is seen that they display a thermal conductivity much lower in magnitude and vastly different in temperature dependence. $K \propto T^2$ at low temperatures, passes through a plateau between 5 and 15K and then again increases with temperature. The first attempt at an interpretation of these features was made by Kittel[38] who used equation (2) to analyse the data for a few glasses above 40K. For vitreous silica it was shown that while $l \simeq$ constant $\simeq$ 7 Å above 200K, it increases at lower temperatures reaching 15 Å at 40K. If a glass is considered as a continuous random network, then at high temperatures where the wavelength of the dominant phonons is short, one would expect scattering at the boundaries of the unit cells thus leading to a constant mean free path of the order of the size of a unit cell. As the temperature is reduced the wavelength of the dominant phonons becomes much larger than the scale of the microscopic disorder (a few Å), so the amorphous medium becomes essentially an elastic continuum and the details of the atomic structure is unimportant. In this region, the scattering of phonons becomes weaker, and the phonon mean free path is longer than the wavelength of the dominant phonons which in turn is larger than the dimension of the microscopic disorder. *Figure 2* shows that this condition is indeed satisfied below about 100K and an amorphous solid can then be treated by means of the same theory as a crystalline solid[15,39]. Even in the phonon picture two different approaches have been proposed and these will be discussed in turn.

Phonon scattering by disordered structure

Klemens[39] made the first attempt at an interpretation of the thermal conductivity of amorphous solids over a wide temperature range by assuming that the scattering of phonons is due to the elastic disorder of the amorphous structure and this is termed 'structure scattering'. A plausible argument was presented to show that at low frequencies the mean free path l for this process is proportional to ω^{-2}. Ziman[40] has refined this calculation by using techniques developed for

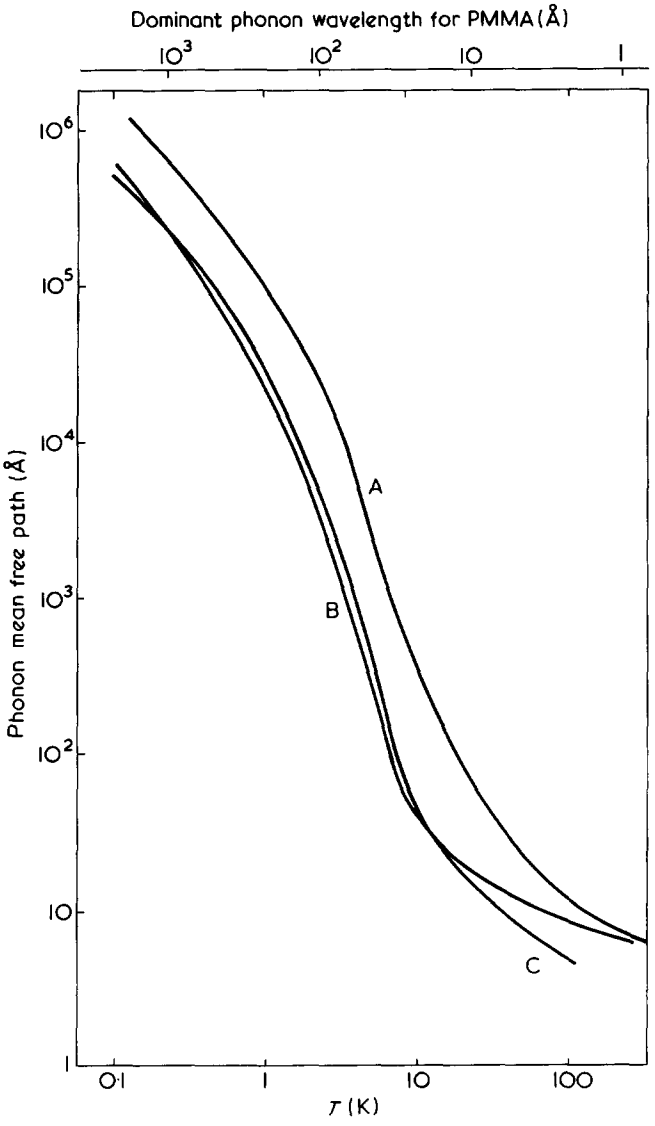

Figure 2 Average phonon mean free path $l(T)$ after (2) for amorphous SiO_2, Se and PMMA. The values for SiO_2 and Se are taken from ref 14 while those for PMMA are calculated from the thermal conductivity in *Figure 1* and the acoustic heat capacity obtained by Reese (ref 9) from the Tarasov model. A, SiO_2; B, PMMA; C, Se

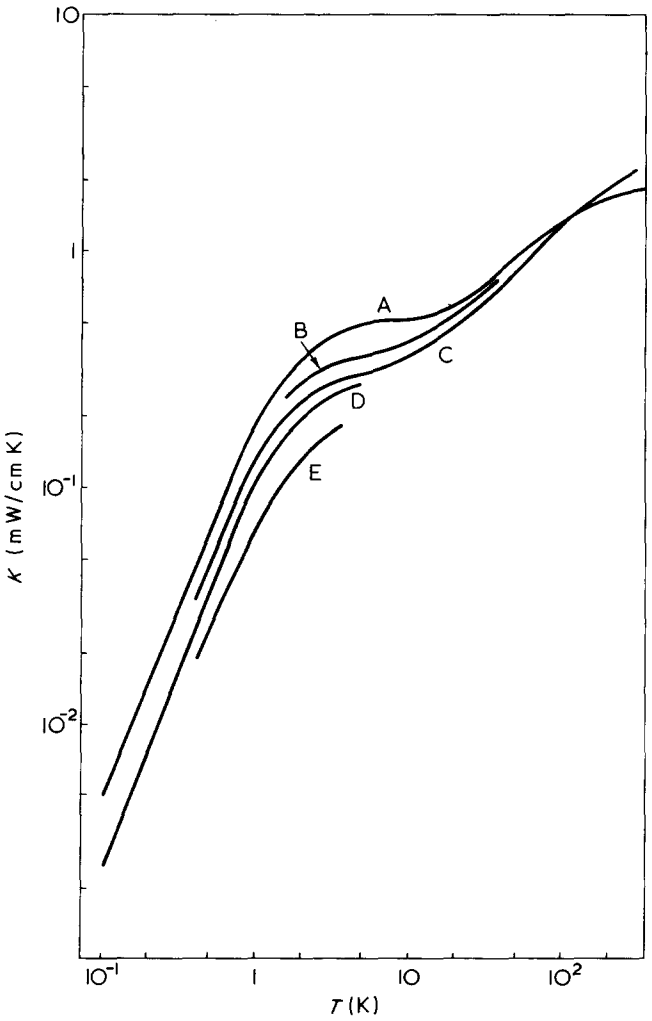

Figure 3 Thermal conductivity of amorphous polymers. The data for PMMA, poly(ethylene terephthalate) (PET), polycarbonate (PC), polystyrene (PS) and poly(vinyl acetate) (PVAc) are taken from refs 2 to 13. A, PMMA; B, PET; C, PC; D, PS; E, PVAc

the treatment of the propagation of radio waves through an irregularly refracting ionosphere. The mean free path is then given by:

$$l = B\omega^{-2} \quad \text{for} \quad \frac{v}{\omega a'} \gg 1 \tag{3a}$$

$$l = \text{constant for} \quad \frac{v}{\omega a'} \leqslant 1 \tag{3b}$$

where B is a constant characterizing the material, a' is the scale of the microscopic disorder and v/ω is the wavelength of the phonons.

The result of l = constant at high temperatures gives rise to $K \propto C$ and thus K will increase slowly with temperature. This is consistent with the experimental data for all amorphous solids and in particular, for amorphous polymers, as illustrated in *Figures 3* and *4*. Furthermore, l is found to be about 7 Å for all these polymers (*Figure 2*). However, the substitution of equation (3a) into equation (2) gives $K \propto T$ at low temperatures, which disagrees with the observed T^2 dependence.

A modification to the above model has also been proposed by Klemens[15] who assumes that the amorphous structure gives rise to spatial fluctuations in the sound velocity which in turn leads to the scattering of phonons. The sound velocity can thus be written as $v + s(\vec{x})$, where v is the average sound velocity and $s(\vec{x})$ is the local fluctuation from the average. Then, using perturbation theory and ignoring the difference between longitudinal and transverse waves, the relaxation time τ (= l/v) for the scattering of a phonon with wavevector $\vec{q}$ into other states is given by:

$$\tau^{-1} = \frac{3V}{(2\pi)^2 M^2} \int ds' \frac{c^2(\vec{q},\vec{q}')}{v\omega^2} \left[1 - \frac{\vec{t}\cdot\vec{q}'}{\vec{t}\cdot\vec{q}}\right] \tag{4}$$

where V is the volume of the solid, the integration is over the surface $\omega = \omega'$ in $\vec{q}'$ space and $\vec{t}$ is the unit vector in the direction of the temperature gradient; $c(\vec{q},\vec{q}')$ can be expressed as:

$$c(\vec{q},\vec{q}') = \frac{2Mv}{V} q\, q' \int d\vec{x}\, s(\vec{x}) \exp(i\vec{p}\cdot\vec{x}) \tag{5}$$

where $\vec{p} = \vec{q}' - \vec{q}$ and the integration is over the volume of the solid.

One can then introduce two quantities to describe the ran-

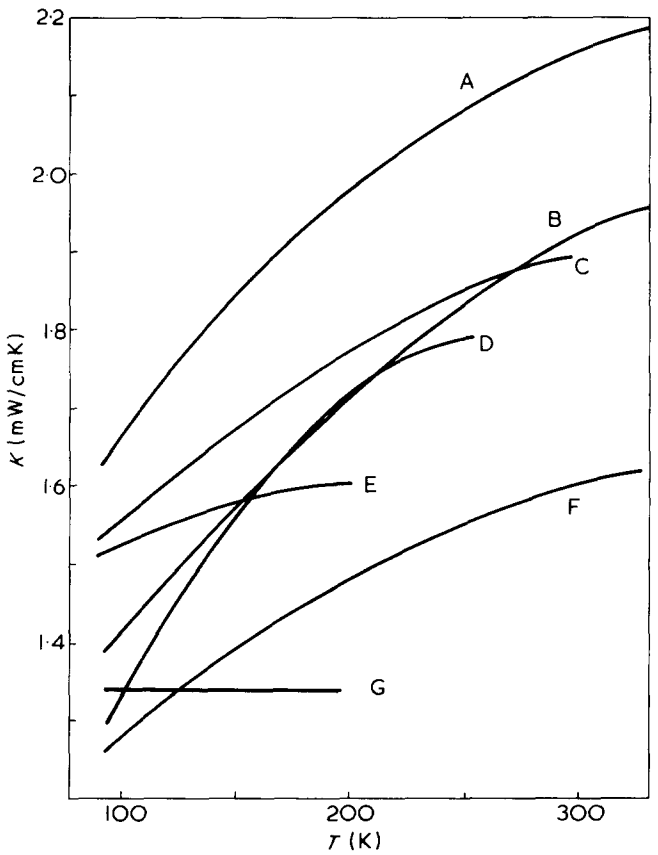

Figure 4 Thermal conductivity of amorphous polymers above 100K. Data for PET, poly(ethyl methacrylate) (PEMA), poly(n-butyl methacrylate) (PBMA), atactic polypropylene (PP), natural rubber, poly(vinyl chloride) (PVC) and polyisobutylene (PIB) from refs 2 and 41. Only data below the glass transitions are shown. Above the transitions the slopes of the curves change to negative. A, PET; B, PEMA; C, PBMA; D, PP; E, natural rubber; F, PVC; G, PIB

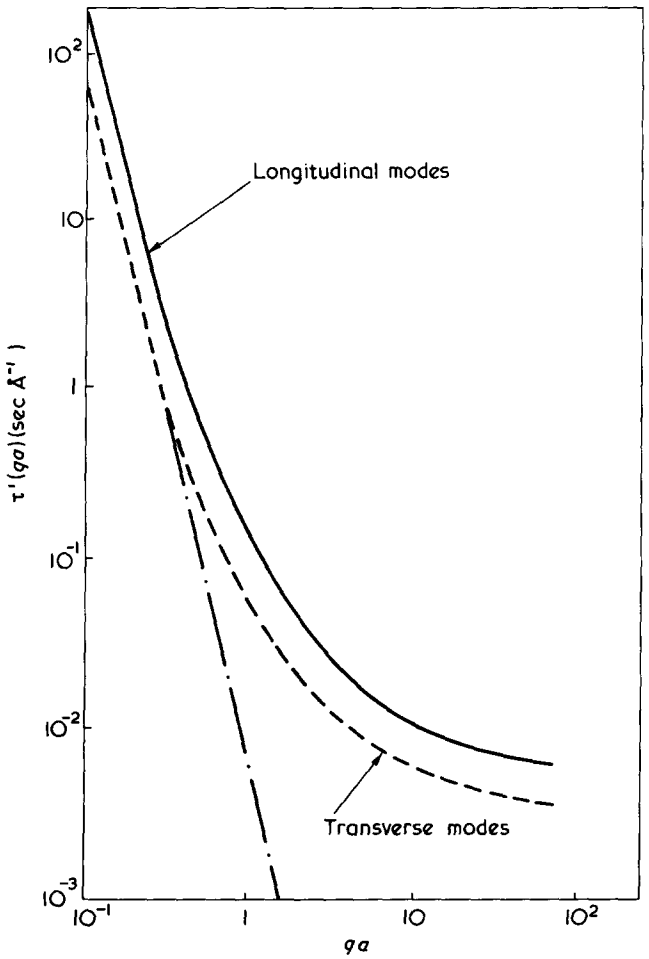

Figure 5 The relaxation times from the model of Morgan and Smith (ref 16). $\tau' = \tau \times 10^{12}\Delta^2 v_L/a v_n$, $v_L = 2v_T$ and $v_n = 4 \times 10^3$ m/sec, where v_L and v_T are the longitudinal and transverse velocities of phonons. The straight line corresponds to the long wavelength form, for transverse modes, extrapolated to short wavelengths

dom fluctuations in the velocity: the mean square fluctuation:

$$\langle s^2 \rangle = \frac{1}{V}\int d\vec{x}\,[s(\vec{x})]^2 \tag{6}$$

and the spatial correlation function:

$$f(\vec{r}) = \frac{1}{V\langle s^2\rangle}\int d\vec{x}\, s(\vec{x})s(\vec{x}+\vec{r}) \tag{7}$$

If one defines the structure factor:

$$\phi(\vec{p}) = \int d\vec{r} f(\vec{r})\exp(i\vec{p}\cdot\vec{r}) \tag{8}$$

and assumes that $f(\vec{r})$ and hence $\phi(\vec{p})$ are spherically symmetric, then:

$$\tau^{-1}(q) = \frac{6}{v}\langle s^2\rangle \int_0^{2q} p^3\phi(p)dp \tag{9}$$

Thus the frequency dependence of τ is determined by the p dependence of $\phi(p)$ and the strength of the scattering is also governed by the factor $\langle s^2 \rangle$.

Since there is very little information on the form of the structure factor $\phi(p)$ for amorphous polymers we will not consider the application of equation (9) to these substances. However, in later sections on semicrystalline polymers, Klemens' theory will be used to describe the additional phonon scattering arising from the presence of crystallites.

Following this idea that phonon scattering is caused by the spatial fluctuations in sound velocity, Morgan and Smith[16] have developed a microscopic model of elastic scattering. It is assumed that $f(\vec{r}) = \exp(-r/a)$, where a is termed the correlation length, while another quantity Δ^2 is used as a measure of the magnitude of the velocity fluctuations. The relaxation times for the longitudinal and transverse waves have been evaluated, the results of which are reproduced in *Figure 5*.

The calculation of the thermal conductivity is now straightforward. But since $\tau \propto q^{-4}$ when $qa \ll 1$ the calculated thermal conductivity will become infinite unless another scattering mechanism is introduced to limit the mean free path of the low-frequency phonons. Assuming this mechanism to be boundary scattering, the thermal conductivity can be calculated by using a total mean free path $l^{-1} = l_b^{-1} + l_e^{-1}$, where l_b denotes the size of the sample and l_e is the mean free path due to elastic scattering. The results are shown in *Figure 6* (using parameters appropriate to amorphous Se) for different values of a. For large values of a (1000–3000 Å) $K \propto T^n$ where $2 < n < 3$ in the range

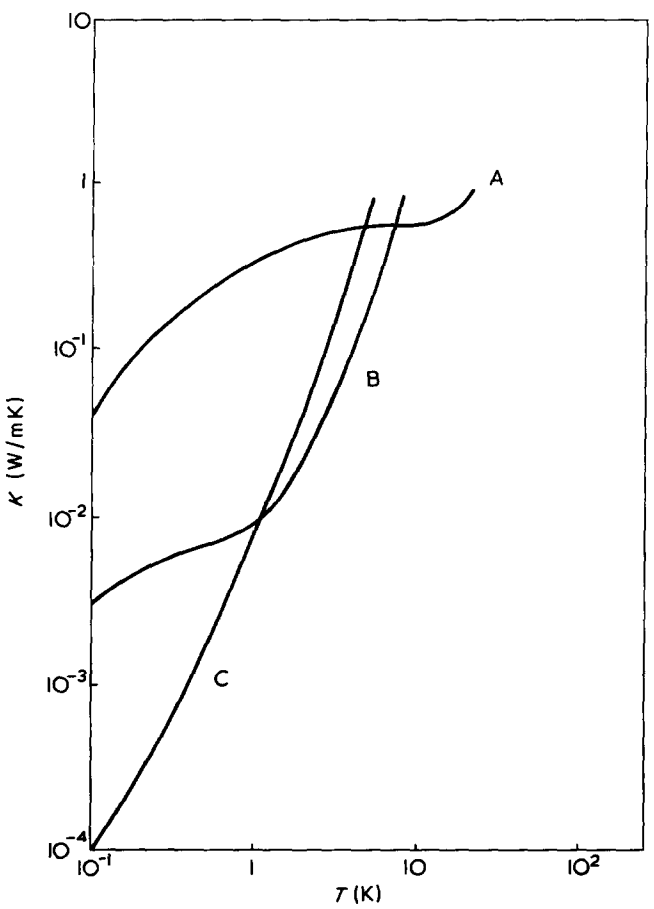

Figure 6 The thermal conductivity as a function of temperature for different values of a. $\Delta^2 = 0.01$, $l_b = 10^{-2}$m and the other parameters correspond to amorphous Se. Data from Morgan and Smith (ref 16). A, a = 15 Å; B, a = 100 Å; C, a = 3000 Å

0.1 to 1K. When a is reduced to 500–100 Å K becomes flat at very low temperatures until finally a plateau develops when a is sufficiently small (15–5 Å). This suggests that the temperature dependence of K of amorphous solids may be explained in terms of long- and short-range correlations existing simultaneously. *Figure 7* shows the fit to the data of Se obtained by Morgan and Smith, using the values $\Delta_L{}^2 = 5 \times 10^{-4}$, $a_L = 3000$ Å, $\Delta_s{}^2 = 4 \times 10^{-1}$, $a_s = 8$ Å, where the subscripts L and s denote the long-range and short-range correlations. We will not use this model to fit the data on amorphous polymers but merely note that, with appropriate choice of the 4 parameters, reasonable agreement can certainly be obtained.

The principal justification for this model lies in the fact that light scattering experiments do indicate long correlation lengths of about 3000 Å in some amorphous materials[16]. Whether long-range correlations exist in all amorphous solids is still an open question and in this respect, more light scattering and thermal conductivity measurements on the same samples will be useful. It should be noted that the Morgan–Smith model is also applicable to semicrystalline polymers if we introduce an additional correlation length of the size of the crystallites ($\simeq$ 100 Å) and the detail of this treatment will be discussed later.

Resonant scattering of phonons

A completely different kind of model, which assumes resonant scattering of phonons by tunnelling states, has been independently suggested by Anderson *et al.*[17] and Phillips[18]. According to this model, certain atoms or groups of atoms in an amorphous solid can occupy two different positions corresponding to the minima of double-well potentials (*Figure 8*). A small asymmetry ϵ in the depth of the potential wells exists because the surrounding of the particles in position 1 is slightly different from that of position 2. Even though at low temperatures the particle does not have sufficient energy to surmount the barrier, yet it can move from one minimum to the other through phonon-assisted tunnelling.

If we assume that the zero-point energy $\hbar\omega_0$ of the motion of the particle around the minimum is the same in both positions then the two lowest energy states of this asymmetric double-well is $E = \pm(\epsilon^2 + \alpha^2)^{1/2}$, where the coupling energy is $\alpha = \hbar\omega_0 \exp(-\mu)$ and μ is roughly proportional to the distance $\bar{d}$ between the two minima and to the square root of the barrier height $\bar{V}$. The parameters ϵ and μ are assumed

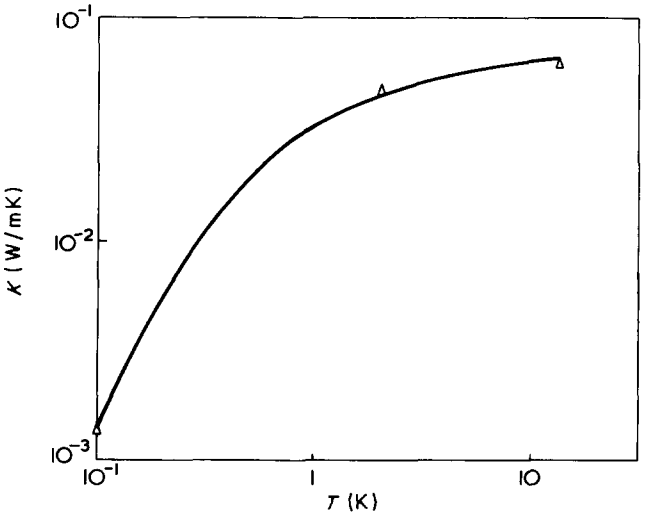

Figure 7 Theoretical fit to the data of amorphous Se. Data from Morgan and Smith (ref 16)

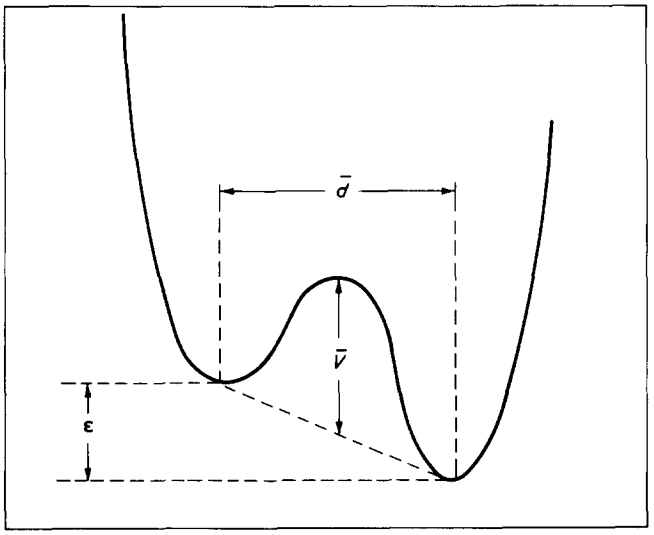

Figure 8 Asymmetric double-well potentials

to be uniformly distributed in the range important at low temperature, leading to a probability distribution $P(\epsilon,\mu) = \bar{P}$, where $\bar{P}$ is a constant.

The interaction between this two-level system and the phonons arises from the deformation of the double-well potential by an elastic wave. When the phonon energy is near or equal to the energy difference of the two levels it will be absorbed and then incoherently re-emitted. The phonon mean free path is then given by $l \propto \omega^{-1} \coth(\hbar\omega/2kT)$, which is approximately ω^{-1} at sufficiently low temperature. Therefore, using equation (2) $K \propto T^3 T^{-1} = T^2$, which agrees with the observed temperature dependence. The tunnelling model of an amorphous material has received considerable support from its success in predicting the observed linear temperature dependence in the specific heat[12,14], the saturation properties of the ultrasonic absorption[42,43], and the anomalies in the sound velocity[44] and thermal expansion[45]. However, this model by itself gives no indication of the nature of the tunnelling states, nor the reason why the thermal properties of amorphous solids have such similar magnitude and temperature dependence. While spectroscopic methods are potentially powerful in the investigation of these states, so far they have not been too successful[14], probably because of the broad distribution in the level spacings.

At slightly higher frequencies, in the range of θ ($=\hbar\omega/k$) between 5 and 20K, another resonant scattering mechanism has been proposed[19]. This is based on the observation that the measured specific heat[13,46–50] is in excess of the acoustic value deduced from sound velocities, suggesting the existence of another band of localized vibrational modes. The particles contributing to these modes are assumed[51] to be situated in or near cavities, thus only weakly coupled to the lattice. They will then vibrate almost independently and hence strongly absorb phonons having the right frequency.

Combining these ideas, we can thus divide the frequency spectrum into three regions.

(a) $\omega \leqslant \omega_R$, $l = D\omega^{-1}$ *

* If the expression $l \propto \omega^{-1} \coth(\hbar\omega/2kT)$ is used, then the saturation of the two-level system at high temperatures would lead to unrealistically long phonon mean free path for the low-frequency phonons, and other scattering mechanisms would have to be included[52]. Because of the primative state of the model we will not consider this refinement.

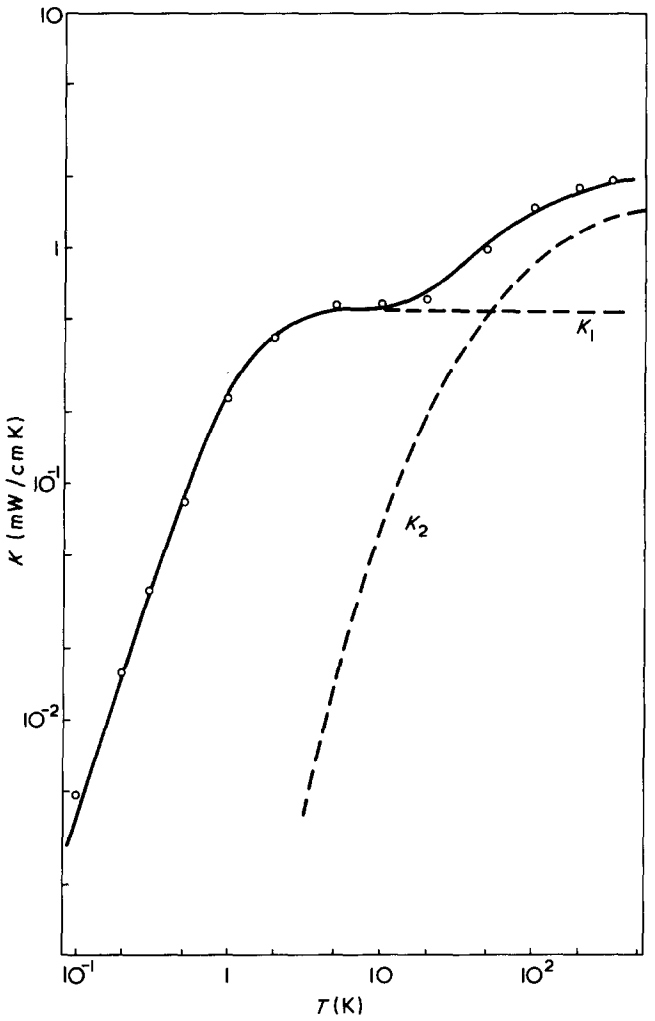

Figure 9 Theoretical fit to the data of PMMA according to equations (10) and (11). The points are data from *Figure 1*

where ω_R is the lower limit of the band of localized vibrations. Substituting this $l(\omega)$ into equation (1) the contribution of the phonons in this frequency region is:

$$K_1 = \frac{k^3 D}{2\pi^2 \hbar^2 v^2} T^2 \int_0^{\theta_R/T} \frac{x^3 e^x}{(e^x - 1)^2} \, dx \qquad (10)$$

where $\hbar$ is Planck's constant, k is Boltzmann's constant, $\theta_R = \hbar\omega_R/k$ and $x = \hbar\omega/kT$. Here the Debye spectrum is used, i.e. the density of acoustical modes is proportional to ω^2 and the integral includes contributions of both transverse and longitudinal waves.

(b) $\omega_R < \omega \leqslant \omega_C$

where ω_C is the upper limit of the band of localized vibrations. This is the region where the mean free path is expected to be small (of the order of interatomic distances) because of strong phonon scattering by the band of localized vibrations.

(c) $\omega_C < \omega \leqslant \omega_1$

where ω_1 is the maximum frequency of the acoustic phonon spectrum. In this region of high frequencies we know from both Ziman's theory[40] and the experimental data that $l \simeq$ constant $\simeq$ a few Å. In order to reduce the number of parameters we equate the mean free paths in regions b and c and so the total contribution from these two regions is:

$$K_2 = \frac{1}{3} vl \int_{\theta_R/T}^{\theta_1/T} g(\omega) \frac{x^2 e^x}{(e^x - 1)^2} \, dx \qquad (11)$$

where $g(\omega)$ is proportional to the density of states of the acoustic modes and $\theta_1 = \hbar\omega_1/k$. We note that both equations (10) and (11) derive from equation (1), but as a result of the difference in frequency dependence of $l(\omega)$ and $g(\omega)$ in the two cases the forms of the integrals are not the same.

For solids with linear chain structure such as the polymers we are considering, it has been shown[53,54] that $g(\omega)$ follows a ω^2 distribution from 0 to a frequency characterized by θ_3 and then becomes constant from θ_3 to the maximum frequency θ_1. The values of θ_3 and θ_1 for poly(methyl methacrylate) (PMMA) have been obtained by Reese[9] so we can apply equations (10) and (11) to analyse the thermal conductivity of this polymer. The results are shown in *Figure 9* and it is clear that there is reasonable agreement throughout the whole temperature range of 0.1 to 350K. The values of the parameters used are $D = 1.35 \times 10^8$ cm/sec, $\theta_R = 4.7$K and $vl = 1.31 \times 10^{-2}$ cm^2/sec. Using $v = 1.79 \times 10^5$ cm/sec from the sound velocity measurements[49] l is found to be 7.2 Å.

In the model we are using, the parameter D is considered to be a constant characterizing the material and θ_R is to be identified with the lower frequency limit of the band of localized vibrations. The value of θ_R is consistent with the result of specific heat measurements which show that the excess contribution can be explained by the existence of non-acoustic modes at frequencies corresponding to 4.9K (θ_a) and 17.5K (θ_b), respectively[49]. The value of 7.2 Å for l is also quite reasonable since the distance between vibrating units on neighbouring chains estimated from the density is 7.5 Å[9,10].

We have applied the same analysis to the low-temperature data of other amorphous polymers and the resulting values of D and θ_R are given in *Table 1*, together with θ's obtained from specific heat measurements. It should be noted that the values of D and θ_R do not vary considerably from one polymer to another, the reason being that, at any temperature, the values of the thermal conductivity of all amorphous polymers lie within a factor of two (see *Figures 3* and *4*). Furthermore, if we consider only the range above 15K, then the thermal conductivity at any temperature is within 15% of the average value. We will see that this important result is very useful when discussing the thermal conductivity of semicrystalline polymers in the next section.

In conclusion, while existing models are able to explain

Table 1 Parameters D and θ_R obtained from the analysis of the low-temperature thermal conductivity of amorphous polymers. Please refer to the text for explanation of symbols

Polymer	$Dx10^{-7}$ (cm/sec)	θ_R(K)	θ_a(K)	θ_b(K)
Poly(methyl methacrylate)	13.5	4.7	4.9	17.5
Polystyrene	6.02	5.2	5.5	16
Polycarbonate	5.61	4.5	5.0	14
Poly(ethylene terephthalate)	5.43	4.3	–	15

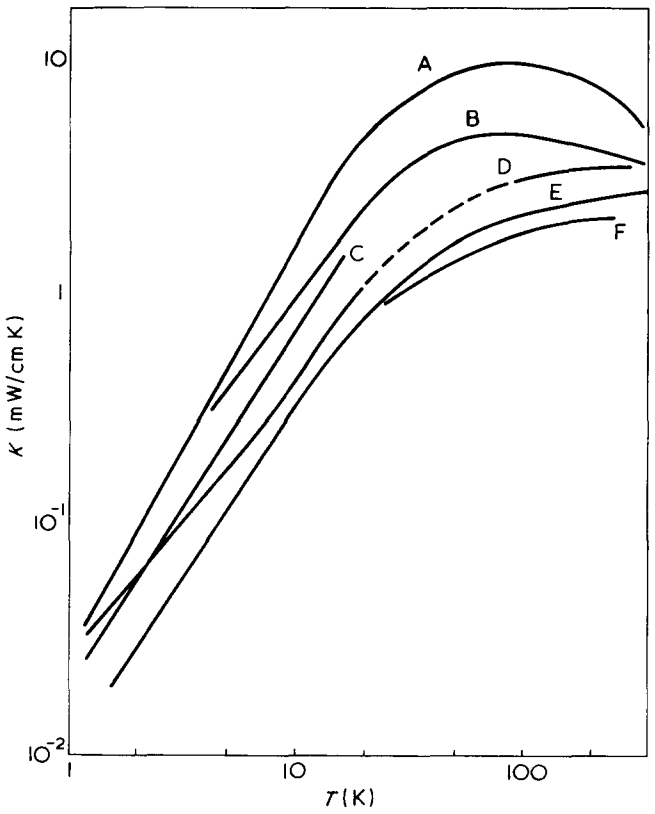

Figure 10 Thermal conductivity of semicrystalline polymers. Data for polyethylene (PE1, $X = 0.81$; PE2, $X = 0.71$; PE4, $X = 0.43$), polyoxymethylene (POM, $X = 0.70$), PET ($X = 0.51$) and isotactic polypropylene (PP, $X = 0.62$) from refs 4, 7, 8 and 22. – – – –, interpolation between existing data. A, PE1; B, POM; C, PE2; D, PE4; E, PET; F, PP

the unusual temperature dependence of the thermal conductivity of amorphous solids further justification of these cannot be obtained from conductivity measurements alone. It is hoped that, with the combination of several techniques such as low-angle X-ray measurements, light scattering and spectroscopic methods, more information about these solids will be forthcoming in order to help us narrow down on a particular model.

SEMICRYSTALLINE POLYMERS

The thermal conductivity of semicrystalline polymers exhibits a temperature dependence vastly different from that of the amorphous ones and this typical behaviour is illustrated in *Figure 10*. No plateau region is observed and the thermal conductivity displays a T^1 and T^3 dependence below 20K. For the highly crystalline (volume fraction crystallinity $X \geqslant 0.7$) polymers such as POM and high density PE the thermal conductivity first increases with increasing temperature, reaches a peak near 100K and then decreases, while for polymers of comparatively low crystallinity such as low density PE, PET and polypropylene (PP) the thermal conductivity increases monotonically up to their respective glass transition temperatures.

It is also seen from *Figure 10* that at high temperatures the thermal conductivity of PE increases significantly with crystallinity but this effect diminishes near 2K. An even better illustration is provided by the data on PET (*Figure 11*) which clearly demonstrate two opposite trends: K increasing with X at high temperature but decreasing with increasing X below 10K. At 1.5K the conductivity of a 50% crystalline sample is more than ten times lower than that of the amorphous one. Since the conductivity of the crystallites is expected to increase with decreasing temperature such unusual behaviour can only arise from an additional phonon scattering mechanism which becomes important at low temperatures.

Before going into any further discussion it is worthwhile to describe briefly the morphology of semicrystalline polymers[55]. Such a material consists of crystalline units called lamellae embedded in an amorphous matrix. The lamellae, with lateral dimensions of the order of 1 μm and thickness of the order of 100 Å, are made up of chains folded back and forth between the lamella surfaces. In an isotropic, melt-crystallized sample the lamellae are randomly oriented and will arrange themselves end-to-end to form ribbon-like structures which grow out from nucleating centres to form larger structures called spherulites. There is also considerable evidence[56–59] that the lamellae are in turn composed of mosaic crystalline blocks of lateral dimensions 100–300 Å, with boundaries defined by dislocations. While the interlamellar amorphous regions and the intermosaic block regions have been termed the amorphous state of the first and second kind, respectively[60], they will be considered identical as a first approximation, so a semicrystalline polymer can be treated as a two-phase material with roughly spherical crystallites.

With this physical picture in mind we can continue our discussion which, for convenience, will be divided into two parts dealing consecutively with the behaviour above and below 30K.

High temperature behaviour

We first consider the region above 30K where the dominant phonon wavelength is much smaller than both the

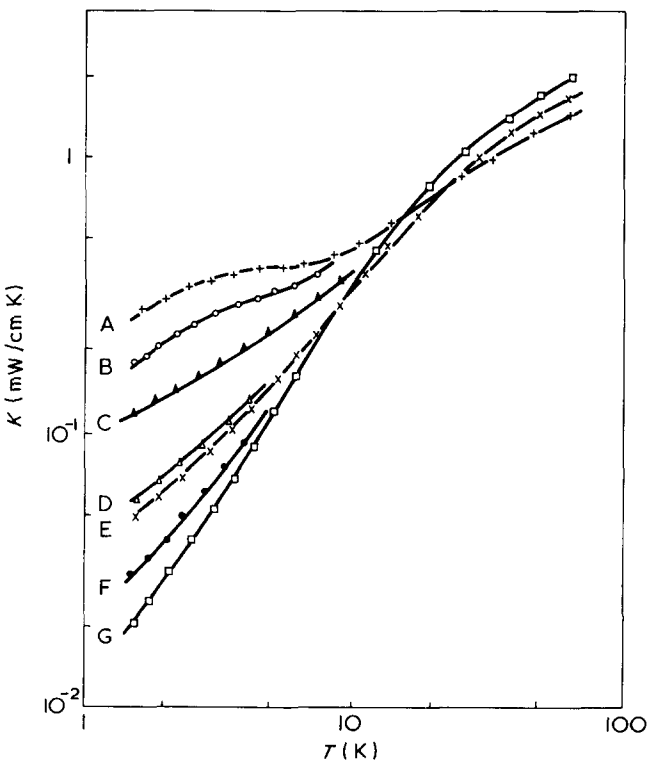

Figure 11 Thermal conductivity of PET. Data from ref 7. A, $X = 0$; B, $X = 0.09$; C, $X = 0.17$; D, $X = 0.25$; E, $X = 0.29$; F, $X = 0.39$; G, $X = 0.51$

crystallite size and the intercrystallite distance, and the boundary resistance is negligible. Here the conductivity of a semicrystalline polymer is expected to depend only on the conductivity of the amorphous and crystalline regions, respectively, the crystallinity X and the shape of the crystallites. It is therefore not too surprising that early analyses by Eiermann[4] and Sheldon and Lane[61] of the crystallinity dependence on the basis of the Maxwell model seem quite successful since this model considered isotropic spherical inclusions randomly distributed in a matrix and treated the mutual interaction among them in an average manner. However, the model is not strictly valid for polymers since the large difference between the intrachain covalent bonding and the interchain van der Waals interaction is expected to give rise to large anisotropy in the intrinsic thermal conductivity of the crystallites. In fact, theoretical estimate[6] shows that the conductivity along the chain direction of a crystallite ($K_{c\parallel}$) is more than 50 times larger than that of the amorphous region (K_a) which is in turn comparable to the conductivity perpendicular to the chain direction ($K_{c\perp}$). This is also experimentally confirmed as we shall see in later sections where oriented polymers are considered.

The Maxwell model has recently been generalized to the case where the inclusions are thermally anisotropic and this provides not only a more realistic description of the crystallinity dependence but also an explanation for the orientation effect[62]. For the moment let us concentrate on isotropic polymer the conductivity of which is given by the model as[62]:

$$\frac{K-K_a}{K+2K_a}=X\left[\frac{2}{3}\frac{k_\perp-1}{k_\perp+2}+\frac{1}{3}\frac{k_\parallel-1}{k_\parallel+2}\right] \tag{12}$$

where $k_\perp = K_{c\perp}/K_a$ and $k_\parallel = K_{c\parallel}/K_a$. Equation (12) will of course reduce to the Maxwell expression when the crystallites are isotropic, i.e. $k_\perp = k_\parallel$. For polymers, however, $k_\parallel \gg 1$ and equation (12) becomes:

$$\frac{K-K_a}{K+2K_a}\simeq X\left[\frac{2}{3}\frac{k_\perp-1}{k_\perp+2}+\frac{1}{3}\right] \tag{13}$$

It is seen from equation (13) that K is almost independent of $K_{c\parallel}$. Moreover, if amorphous samples are available (as in the cases of PET and PP) K_a can also be directly measured. In any case, K_a for *all* amorphous polymers above 30K are so similar (see *Figures 3* and *4*) that it can be easily estimated to within 15%. Therefore the only remaining parameter in equation (13) is $K_{c\perp}$ which can be obtained by the fitting of data. *Figure 12* gives an example of such fits for PE at two different temperatures and the results are quite satisfactory. The resulting $K_{c\perp}$ values for four polymers, shown as functions of temperature in *Figure 13*, fall into two distinct groups with the values for PE and POM decreasing with rising temperature while those for PET and PP being approximately temperature-independent within the accuracy of the analysis. Furthermore, $K_{c\perp}$ of PE follows approximately a T^{-1} dependence, which is characteristic of three-phonon Umklapp scattering processes[37,40]. Its magnitude throughout the whole temperature range is about the same as the thermal conductivity of molecular crystals such as benzene (C_6H_6)[63] which probably possesses van der Waals interaction of similar strength. The much lower $K_{c\perp}$ values for PET and PP are partly the result of weaker interchain van der Waals interactions but the only possible explanation for the gentle temperature dependence seems to be phonon scattering by defects in the crystallites. This is understandable because the repeating units of these two polymers are more complicated and bulky.

Now it is easy to understand the temperature dependence of K above 30K as displayed in *Figure 10*. For polymers with simple structure such as PE and POM $K_{c\perp} \gg K_a$ near 30K, so equation (13) further reduces to $K = K_a(1+2X)/(1-X)$, i.e. K is proportional to K_a and thus increases with rising temperature. However, above 100K where $K_{c\perp}$ and K_a become comparable, K will depend on both these quantities. At high crystallinity ($X \geqslant 0.7$) its temperature dependence is dominated by that of $K_{c\perp}$, so it will decrease with increasing temperature. Therefore, starting from 30K, K first increases, reaches a maximum near 80K and then decreases with temperature. On the other hand, the temperature dependence of K of low-crystallinity ($X \leqslant 0.4$) samples is influenced more by K_a so it will increase with temperature up to about 200K where it exhibits a very shallow maximum (*Figure 14*). For polymers with more complicated structure (e.g. PET and PP) $K_{c\perp}$ is nearly temperature-independent so K has similar temperature dependence as K_a.

Since $K_{c\perp}$ is expected to either increase or remain constant as the temperature decreases equation (13) predicts an increase of K with crystallinity even at low temperatures, in contradiction to the observed behaviour below about 10K. Two models have been proposed to account for this unusual behaviour and we will discuss them in the following sections.

Low temperature behaviour

Correlation in sound velocity fluctuation. The first approach to this problem assumes that the presence of crystallites introduces a correlation length for the sound velocity fluctuation of the order of the size of the crystallites (100 Å). This leads to additional phonon scattering and the accompanying decrease in conductivity. Morgan and Smith[16] have emphasized that this treatment is strictly valid only when the mean free path is larger than the correlation length, so taking amorphous PET as an example and using equation (2), the range of validity is found to be below 5K. Because of its

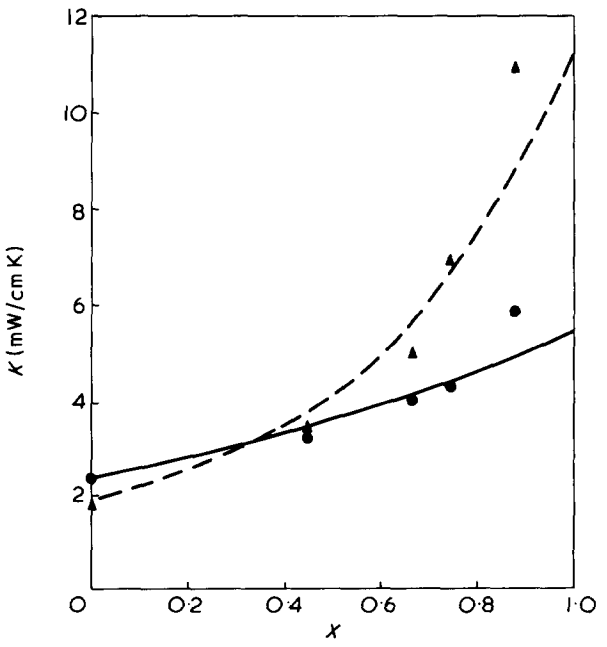

Figure 12 The crystallinity dependence of the thermal conductivity of isotropic PE at 100 and 300K. 300K: ●, data (from ref 4); ——, theoretical. 100K: ▲, data (from ref 4); – – –, theoretical. The theoretical curves are calculated according to equation (13)

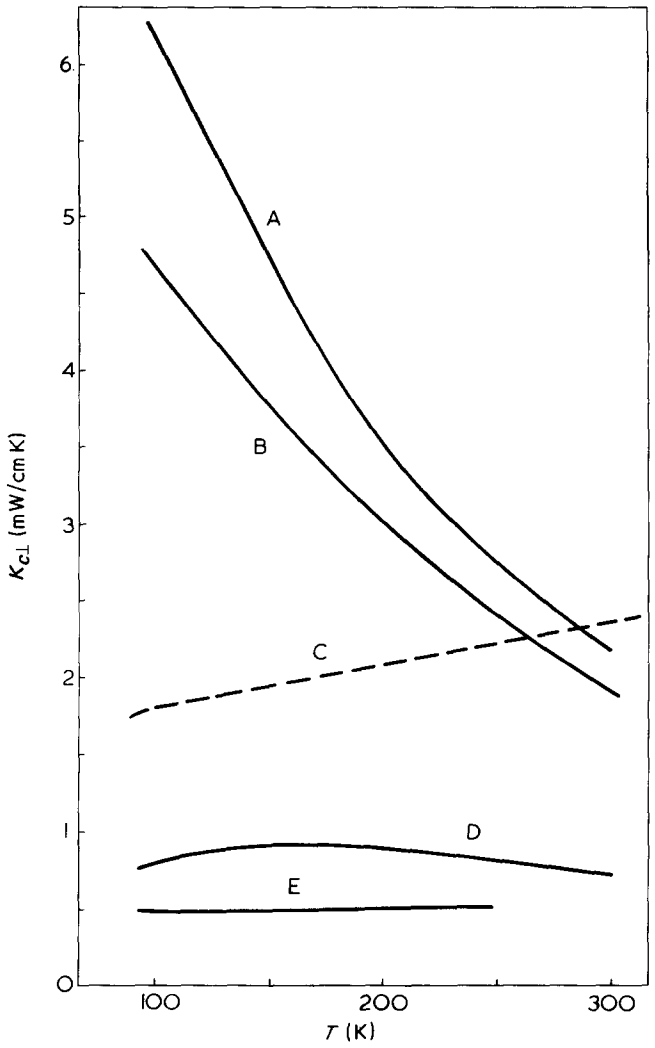

Figure 13 The temperature dependence of the thermal conductivity of the crystallites normal to the chain axis for PE, POM, PET and PP. For comparison we also show K_a, which is the thermal conductivity of amorphous PE obtained by extrapolation of the data for the melt[1]. Its value is typical of *all* amorphous polymers. A, PE; B, POM; C, K_a; D, PET; E, PP

lower conductivity the mean free path in a semicrystalline sample is shorter and this pushes the limit to even lower temperatures.

Based on this idea of an additional correlation length two different attempts have been made to interpret the data for semicrystalline polymers. Assfalg[24] has applied Klemens' theory[15] to analyse the conductivity of PET in the following manner. First, it is assumed that the structure factor for velocity fluctuation $\phi(\vec{p})$ given in equation (8) is proportional to the structure factor for electron density fluctuation $\phi_e(\vec{p})$, which can be obtained from low-angle X-ray diffraction measurements. The maximum in $\phi_e(\vec{p})$ corresponds to Bragg reflection by the periodic density variations arising from the stacking of amorphous and crystalline regions with an average period (the long period) which can be roughly identified with the correlation length. In an isotropic polymer the crystalline lamellae are randomly oriented so $\phi_e(\vec{p})$ has spherical symmetry. Now if we use the dominant phonon approximation, that is, at any temperature T the phonons which contribute most to the thermal conductivity have wavevector $q_d \simeq 4kT/\hbar v$. then the relaxation time in equation (9) becomes $\tau(T) \simeq \tau(q_d) \cong [\phi(q_d)]^{-1}$. Since $\phi(q) \propto \phi_e(q)$ and $l = v\tau$, the thermal conductivity of a semicrystalline sample can be obtained from equation (2):

$$K_s(T) = \frac{[\phi_e(q_d)]_a}{[\phi_e(q_d)]_s} K_a(T) \tag{14}$$

where the subscripts a and s refer to the amorphous and semicrystalline samples, respectively. Therefore, with $\phi_e(q)$ already determined from low-angle X-ray data, $K_s(T)$ can be calculated in terms of $K_a(T)$ and the results are shown in *Figure 15*. It is clear that the main features of the experimental curves, namely, the large decrease of K_s with increasing X, can be reproduced by this model in spite of the crude approximations.

Similar arguments have been employed by Burgess and Greig[6] to explain the data above 2K of both isotropic and extruded PE. It is again assumed that phonons are scattered as they pass through regions of varying sound velocity, i.e. lamellae and amorphous regions, but the Morgan–Smith model[16] is used to obtain a quantitative fit. For heat conduction along the extruded direction the total mean free path can be written as:

$$l^{-1}(q) = l_b^{-1} + l_L^{-1}(q) + (1 - X)l_s^{-1}(q) \tag{15}$$

where $l_L(q)$ and $l_s(q)$ denote the mean free paths for long-range and short-range correlations, respectively, which can be obtained from the universal curves in *Figure 5*. The values of a_L and a_s used are 100 and 8 Å, respectively, and the constant l_b, which is the boundary dimension, is taken to be 1 cm. The l_L^{-1} term accounts for the scattering of phonons arising from velocity fluctuation in alternate regions of amor-

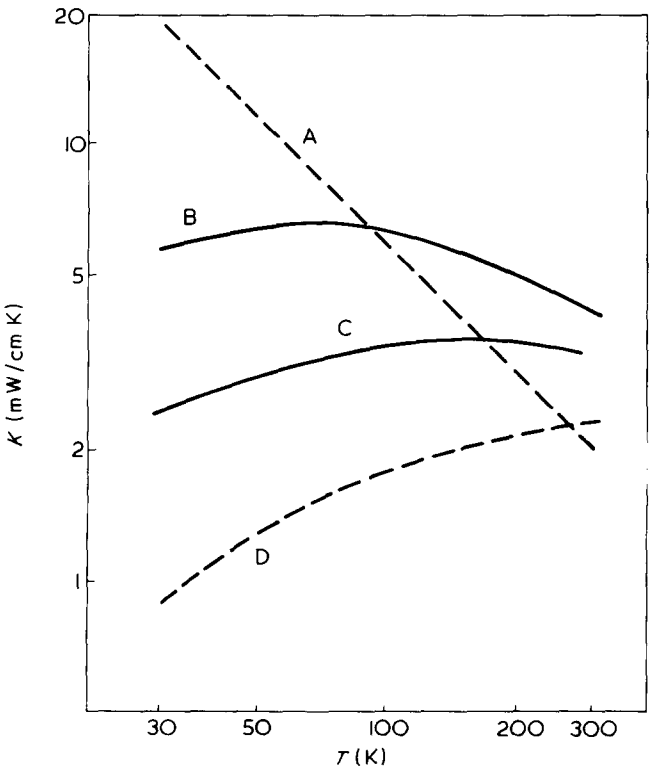

Figure 14 Theoretical thermal conductivity of PE between 30 and 300K at crystallinities X = 0.4 and 0.7. $K_{c\perp}$ below 100K is obtained by extrapolating the roughly $1/T$ curve in *Figure 13* to a lower temperature. K_a is assumed to follow the typical behaviour of amorphous polymers. The theoretical curves at X = 0.4 and 0.7 are calculated according to equation (13). A, $K_{c\perp}$; B, X = 0.7; C, X = 0.4; D, K_a

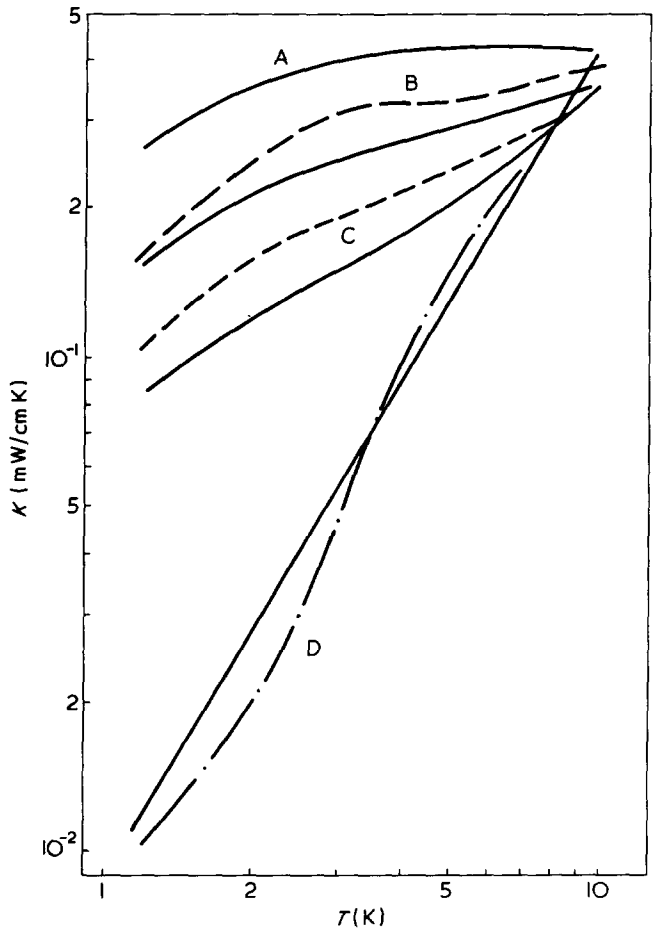

Figure 15 Thermal conductivity of PET between 1 and 10K. ——, experimental data; – – – –, calculated according to equation (14) (from ref 24). A, $X = 0$; B, $X = 0.05$; C, $X = 0.14$; D, $X = 0.75$

phous and crystalline phases, while the term $(1 - X)l_s^{-1}$ is considered to be adequate for describing phonon scattering in the amorphous regions since the effect of the very long correlation length (3000 Å) inherent in amorphous materials is not too important above 2K. Phonon scattering in the crystalline regions is negligible since the chains are already aligned in the extruded direction.

We have formerly mentioned that the model is not valid when the mean free path is smaller than the long correlation length a_L, so the term l_L^{-1} is meaningless for the majority of phonons at high temperatures (near 100K). However, Burgess and Greig[6] have estimated that the effect of neglecting l_L (i.e. setting $l_L^{-1} = 0$) for all phonons at 100K introduces only a 30% difference to the calculated value of K, so the use of equation (15) for the analysis of data in the temperature range of 2 to 100K seems justified.

A good fit to the data is obtained with $\Delta_L^2 = 0.08$ and $\Delta_s^2 = 0.25$ and this is shown in *Figure 16*. Although these parameters are arbitrary it is interesting to note that Δ_s^2 is of the same magnitude as those used by Morgan and Smith for amorphous materials (e.g. Se), which is reasonable since short-range correlation exists only in the amorphous regions of PE. On the other hand, Δ_L^2 is somewhat larger than the corresponding value for amorphous materials, reflecting the large difference in elastic properties between amorphous and crystalline PE.

Equation (15) can also be applied to the data of isotropic PE below 30K where the thermal resistance of the crystallites normal to the chain axis is also negligible compared to that of the amorphous region. Since the lamella thickness (and hence a_L) is roughly the same for isotropic and extruded PE equation (15) predicts similar thermal conductivity for these two samples, in agreement with the experimental data (*Figure 16*). At higher temperature, however, the thermal resistance of the crystallites becomes larger and has to be taken into account. If it is assumed[6] that the amorphous and crystalline regions form a series arrangement in which the crystallites lie with the c-axes all perpendicular to the direction in which K is measured, then equation (15) must be modified to:

$$l^{-1}(q) = l_b^{-1} + l_L^{-1}(q) + (1 - X)l_s^{-1}(q) + Xl_u^{-1}(q) \quad (16)$$

where $l_u(q)$ is the mean free path arising from Umklapp scattering of phonons in the crystallites perpendicular to the c-axis. Although satisfactory fit[6] to the high temperature data can be obtained by employing an appropriate expression for $l_u(q)$ the above assumption on the arrangement of crystallites is not very realistic, and the treatment given in the earlier section on 'High temperature behaviour' seems more appropriate.

Thermal boundary resistance at amorphous–crystalline interfaces. A different model[7] which can also account for the reduction of K with increasing crystallinity assumes that this reduction is caused by the acoustic mismatch between the crystallites and the amorphous matrix which introduces an additional resistance. This thermal boundary resistance R_b depends on the sound velocities and densities of the amorphous and crystalline regions, respectively, and will be

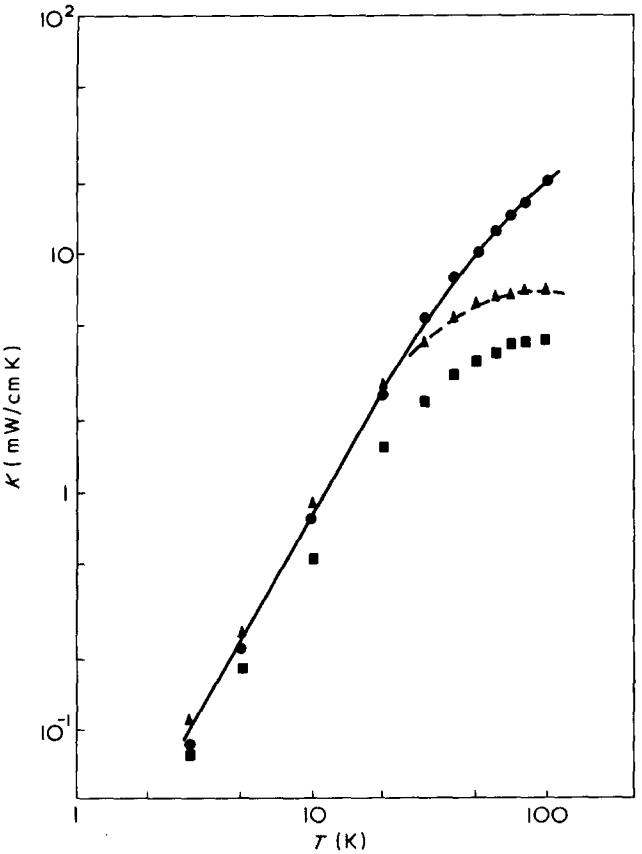

Figure 16 Thermal conductivity of PE (Hostalen GUR, $X \simeq 0.6$). ●, $K_{\parallel}$ data ($\lambda = 4.4$); ——, theoretical (equation 15); ■, $K_{\perp}$ data ($\lambda = 4.4$); ▲, isotropic data; – – – –, theoretical (equation 16)

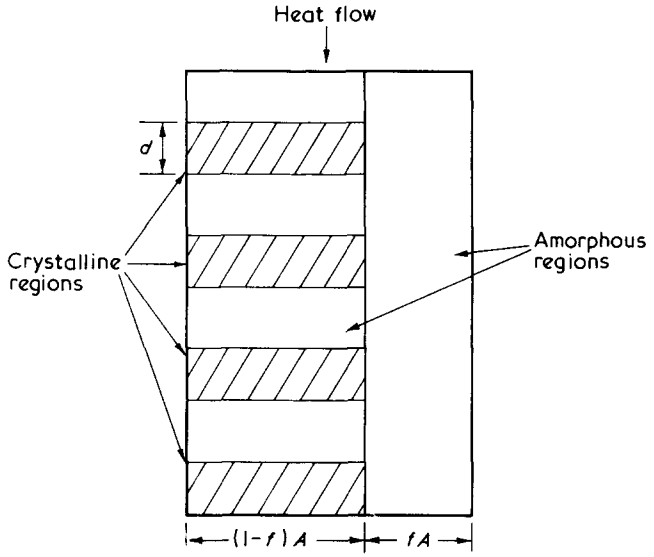

Figure 17 Schematic diagram of the arrangement of amorphous and crystalline regions in isotropic semicrystalline polymers

larger if there is greater disparity in these quantities in the two phases.

This approach receives strong support from the fact that similar behaviour[26,27,64] of the thermal conductivity of composites made from epoxy (an amorphous polymer) with various powder fillers (copper, quartz, corundum etc.) has been successfully explained on the basis of a two-phase model[65] which incorporates thermal boundary resistance. This model takes into account all the relevant factors: the thermal conductivities of the filler and the matrix, the shape, size and concentration of the filler, and the boundary resistance R_b, which are all measurable quantities in the case of composite materials. Unfortunately, it is valid only for dilute concentration of filler (<25%) and though applicable to PET[62], is not useful for other semicrystalline polymers which usually have higher crystallinity. Therefore we have to find another model which holds for a wider range of crystallinity.

In our previous analysis of the high-temperature data the roughly spherical mosaic blocks have been taken as the crystalline inclusions. Now if we consider the limiting case of infinite boundary resistance, which is equivalent to setting both $k_\perp$ and $k_\parallel$ to zero, then equation (12) gives $K = 2K_a(1-X)/(2+X)$, i.e. $K = 0.4\,K_a$ at $X = 0.5$. Since the data for PET at the lowest temperature are much smaller than this value we have to conclude that the low-temperature data are not consistent with spherical crystallites. However, bearing in mind that the effect of boundary resistance is to impede heat flow from the interlamellar amorphous region to both the mosaic and intermosaic regions, it is clear that the basic unit for blocking heat flow must consist of a number of mosaic blocks and thus has a plate-like shape.

A crude description of this physical situation is given by the arrangement in *Figure 17*. That is, for each cross-sectional area A perpendicular to the direction of heat flow, a fractional area fA is completely occupied by amorphous material. In the remaining area, $(1-f)A$, amorphous and crystalline regions are stacked in alternate layers. The thickness d of the crystalline regions represents the effective thickness of the lamellae along the direction of heat flow. Since the lamellae are on average inclined at an angle, say 45°, to the direction of heat flow, d is taken to be $(2)^{1/2}$ times the average lamella thickness of the sample. Assuming linear heat flow through this parallel arrangement of amorphous region and amorphous–crystalline stacks, it is easily shown that:

$$\frac{K}{K_a} = \frac{(1-f)^2}{2XK_a(R_b/d) + (1-f-X)} + f \qquad (17)$$

where the thermal resistance of the crystalline region has been neglected.

Since the average thickness of the lamellae can be obtained from low-angle X-ray diffraction measurements and other methods the application of equation (17) to the analysis of the data of a particular sample requires in general three parameters, f, $R_b(T)$ and $K_a(T)$, where the last two also depend on temperature. For the series of samples of PET (*Figure 11*) for which $K_a(T)$ has also been measured, we are left with only two parameters f and $R_b(T)$. Since $R_b(T)$ cannot be directly measured it has to be estimated from Little's theory[28] which, at sufficiently low temperature, gives $R_b = RT^{-3}$ where R depends on the sound velocities and densities of the amorphous and crystalline phases. Although it has been found experimentally[25–27] that $R_b \propto T^{-n}$ $(2 < n < 2.7)$ between 2 and 5K for a number of materials the theoretical and observed values are normally within a factor of 4 near 3K. Thus Little's expression should be sufficient for indicating whether the present mechanism can possibly account for the observed thermal conductivity.

With the help of equation (17) we can understand qualitatively the unusual features in *Figure 11*. Since crystalline material has a higher average conductivity than amorphous, so at high temperatures where the boundary resistance is negligible, the net conductivity of a polymer always increases with crystallinity. As the temperature decreases R_b increases, so that at some temperature (15–20K in the case of PET), the contribution from R_b more than compensates for any increase in conductivity due to the presence of crystalline regions, thus leading to the cross-over in the thermal conductivity curves. This trend increases until finally, at 1.5K, the conductivity of the 50% crystalline sample is more than ten times less than K_a. The increase in slope of the curves with crystallinity can also be understood as the consequence of combining the resistances due to the amorphous phase and the amorphous–crystalline interfaces. Since experimentally, $K \propto T^{0.5}$ for the amorphous material between 2 and 10K one would expect $K \propto T^\gamma$ (where $0.5 < \gamma < 3$) for the semicrystalline samples. As the crystallinity increases, there will be more interfaces available for scattering of phonons, so the contribution of R_b $(\propto T^{-3})$ becomes more important. Quantitative fit of the data to equation (17) has also been obtained[7] and the results show that $f \simeq 0.1$ for $X > 0.3$, indicating that even at such low X most of the area perpendicular to heat flow is already blocked by the plate-like crystalline units.

We note that PET is particularly suitable for the above analysis because its crystallinity can be changed over a wide range (0.6 to 0 i.e. including the amorphous state) throughout which relevant data are available. The extension of this method to other polymers is much more difficult, mainly because bulk samples of most semicrystalline polymers cannot be transformed into a state of sufficiently low crystallinity (say 0.1) even by fast quenching from the melt. For an example, let us consider PE, which has a reasonably wide crystallinity range and Kolouch and Brown[19] have measured the thermal conductivity of 4 samples (X from 0.43 to 0.81) between 1.2 and 20K (*Figure 18*). The fitting of these data

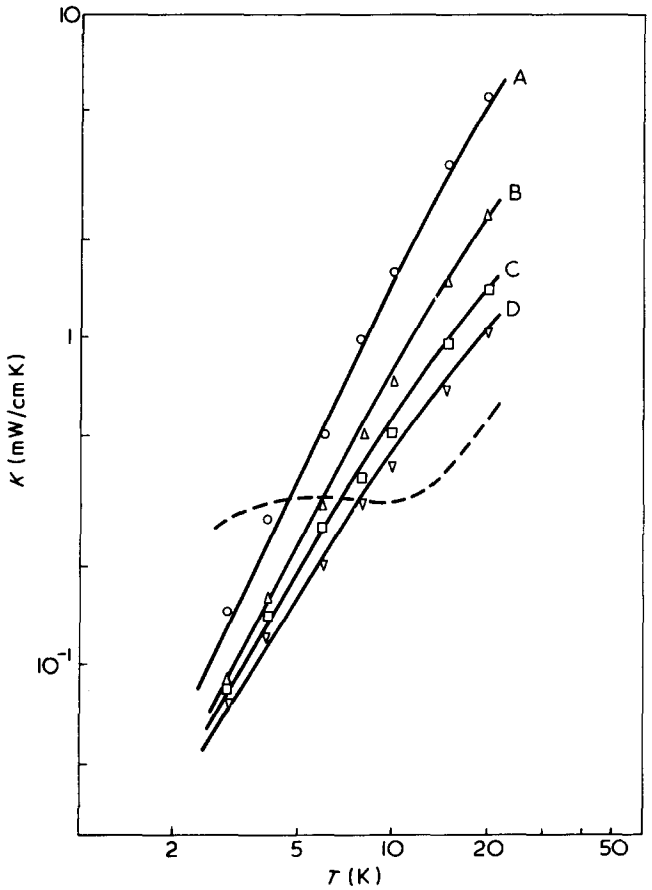

Figure 18 Theoretical fit to the low-temperature data of PE. ——, calculated according to equation (17); – – – –, $K_a(T)$ resulting from data fitting. The points are the smoothed data from ref. 22 and the crystallinities of PE1 to PE4 are 0.81, 0.71, 0.56 and 0.43, respectively. A, PE1; B, PE2; C, PE3; D, PE4

will require more parameters than for the case of PET. To simplify this problem we adopt the following procedure. First, we consider only the data above 3K, where the fit is expected to be relatively insensitive to small variation in f, so that, following the example of PET, it could be taken as 0.1 for all samples. Secondly, the relation $R_b = RT^{-3}$ is assumed to hold for the whole temperature range. Because PE has a high Debye temperature[54] this assumption is certainly justified up to 10K, whereas above this temperature, R_b has dropped to such low values that a slight error in the temperature dependence should have little effect on the result. Finally, $K_a(T)$ for PE is assumed to have the characteristic temperature dependence of amorphous solids, that is, it is temperature-independent between 4 and 10K, while outside this range, it is a slowly varying function of temperature. The lamella thickness of the PE samples has also been obtained by Kolouch and Brown from low-angle X-ray measurements so the values of d are known. From the theoretical curves shown in *Figure 18*, we see that the results are quite satisfactory since the agreement with data is within 10% for all four samples and the $K_a(T)$ obtained from data fitting has similar values as other amorphous polymers.

Data for other polymers are usually available only for a single sample. *Figure 19* shows that the curves fall into two main groups, with the highly crystalline samples (PE1 and POM) having much higher thermal conductivity and a larger slope. It is somewhat surprising to see that the thermal conductivities of four different polymers (PE4, PP, nylon-6,6, PET) of similar crystallinity (X = 0.4 to 0.6) and within 30% of one other. This implies that the value of R_b/d is roughly the same and since for all these polymers of low crystallinity the lamella thickness is about 100 Å, R_b also should not vary to any extent. This point is further illustrated by fitting the data at 4K to equation (17), taking f = 0.1 and K_a = 0.38 mW/cm K (average of the values for several amorphous polymers). The values of the parameters d and R (= R_bT^3) are given in *Table 2*. It is now clear that the unusually large thermal conductivity of polychlorotrifluoroethylene (PCTFE) is the consequence of having larger lamella thickness, and the smaller slope of the curve reveals that it has a low crystallinity (X = 0.34). The crystallinity of the polytetrafluoroethylene (PTFE) sample is not known but the high thermal conductivity probably results from both high crystallinity and large lamella thickness. We also note the absence of a plateau on the curve for poly(vinyl chloride) (PVC) even though this polymer is usually considered amorphous. Actually, PVC has been found[8,66] to contain a small percentage of crystalline regions and we see that the magnitude and temperature dependence of K of this polymer is similar to those of PET of crystallinity of about 0.1 (compare with *Figure 11*). Thus the low-temperature behaviour of all semicrystalline polymers is consistent with the series/parallel model with boundary resistance.

Therefore we conclude that while the modified Maxwell model can satisfactorily account for the behaviour of K

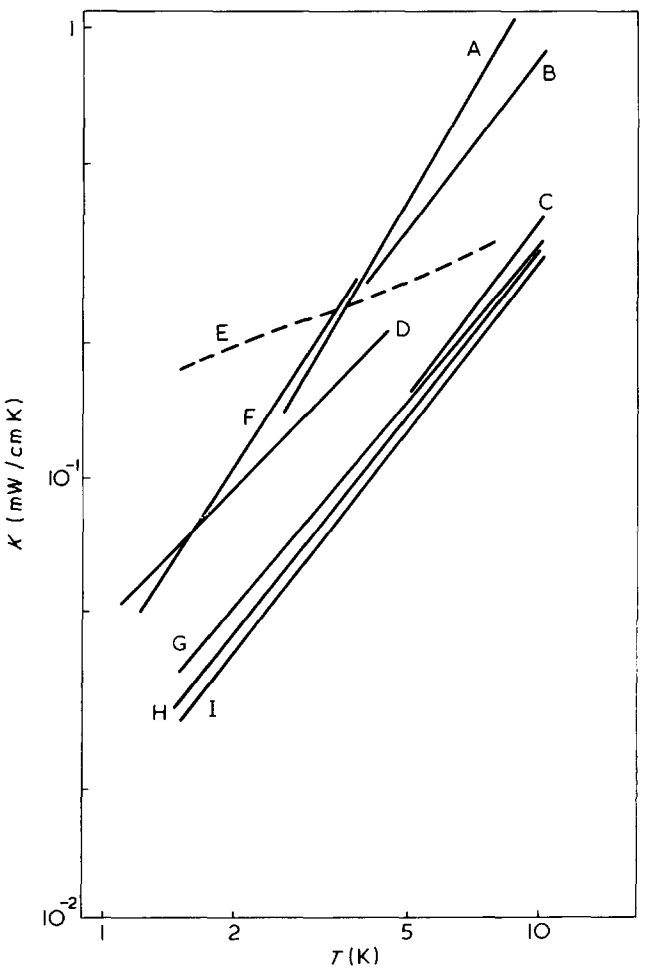

Figure 19 Thermal conductivity of semicrystalline polymers below 10K. Data from refs 7, 8, 21 and 22. A, PE1; B, POM; C PE4; D, PCTFE; E, PVC; F, PTFE; G, PP; H, nylon-66; I, PET

Table 2 Parameters obtained from the analysis of the low-temperature thermal conductivity of semicrystalline polymers. $d = (2)^{1/2} \times$ average lamella thickness. For the samples of PE1 and nylon-66 the lamella thickness given are the measured values[22] while the rest are just typical values obtained from literature[55]. Refer to the text for explanation of other symbols

Polymer	X	K_a (mW/cm K)	d(Å)	$R/d \times 10^{-2}$ [(mW)$^{-1}$ cm K]	$R \times 10^4$ [(mW)$^{-1}$ cm^2 K]
Polyethylene (PE1)	0.81	0.32	282	1.95	5.5
Polyethylene (PE4)	043	0.32	113	4.9	5.5
Polyoxymethylene	0.71	0.38	282	1.27	3.6
Polypropylene	0.57	0.38	170	5.0	8.5
Nylon-66	0.42	0.38	145	7.5	10.8
Poly(ethylene terephthalate)	0.39	0.375	141	8.7	12.2
Polychlorotrifluoroethylene	0.34	0.38	282	3.2	9.1

above 30K there are two physically plausible mechanisms, namely, thermal boundary resistance at amorphous–crystalline interfaces and phonon scattering arising from correlation in sound velocity fluctuation, which can explain the behaviour at lower temperatures. Although the existence of thermal boundary resistance R_b between two materials of different elastic properties is well established, and similar low-temperature behaviour in two-phase composites has been quantitatively accounted for on the basis of a model incorporating boundary resistance, the extension of this analysis to semicrystalline polymers is not straightforward since R_b is not directly measurable and has to be estimated from theory or treated as an adjustable parameter. The models which consider correlation in sound velocity fluctuation are beset by similar problems since they also involve either arbitrary parameters (such as Δ_L^2, Δ_S^2, a_S) or crude assumptions. However, it seems fair to say that we can now understand at least semiquantitatively why, at sufficiently low temperatures, the thermal conductivity of a semicrystalline polymer is always lower than that of its amorphous counterpart.

EFFECT OF ORIENTATION

Amorphous polymers

When an amorphous polymer is uniaxially drawn the chain molecules will tend to align along the draw direction. Since the covalent bonds along the chains are much stronger than the interchain van der Waals forces we would expect the thermal conductivity along the draw direction ($K_{//}$) to be higher than that in the perpendicular direction ($K_\perp$). This anisotropy has been investigated[29–32] for a number of polymers at room temperature and for PMMA between 90 and 300K, the results of which are summarized in *Figure 20*. Since these data have already been discussed in detail in previous reviews[1] we will concentrate only on those aspects which have bearing on our future discussion on semicrystalline polymers.

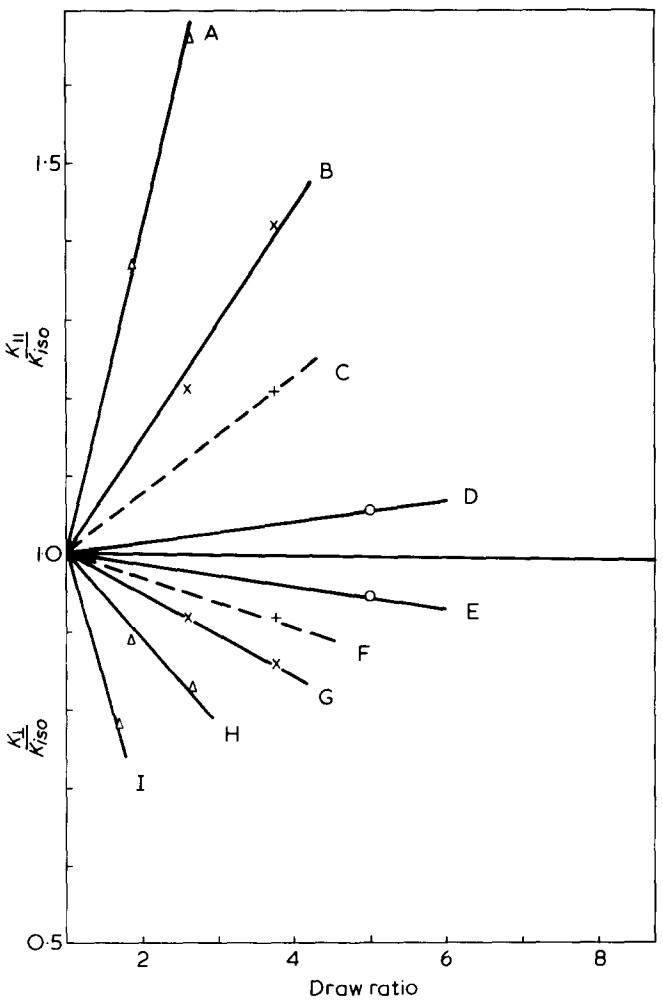

Figure 20 Thermal conductivity of amorphous polymers as a function of draw ratio. — — —, Data at 100K. All other data are at room temperature. (Data from ref 1). A, PVC; B, PMMA; C, PMMA (100K); D, PS; E, PS; F, PMMA (100K); G, PMMA; H, PVC; I, PC

Figure 20 shows that the anisotropy of the thermal conductivity of oriented amorphous polymers in the range of draw ratio (1 to 5) studied is rather small for PS and PMMA but somewhat larger for PVC. This may be related to the fact that PVC normally contains a small fraction ($\simeq$ 10%) of crystalline regions[8,66] which provide very little thermal resistance along the draw direction once the chains are aligned.

Two models have been proposed to explain the effect of orientation. In the first model[31] an unoriented polymer is regarded as a random aggregate of axially symmetric units whose thermal conductivities were those of the fully oriented materials. When the polymer is drawn the units of the aggregate would be aligned with the units themselves remaining unchanged. The thermal conductivities of the partially oriented polymer can be obtained either by using the series or the parallel model. The series model assumes uniform heat flux throughout the aggregate, which implies a summation of thermal resistivities, while the parallel model assumes uniform temperature gradient thus leading to a summation of thermal conductivities. Using the series model the thermal conductivities are given by[31]:

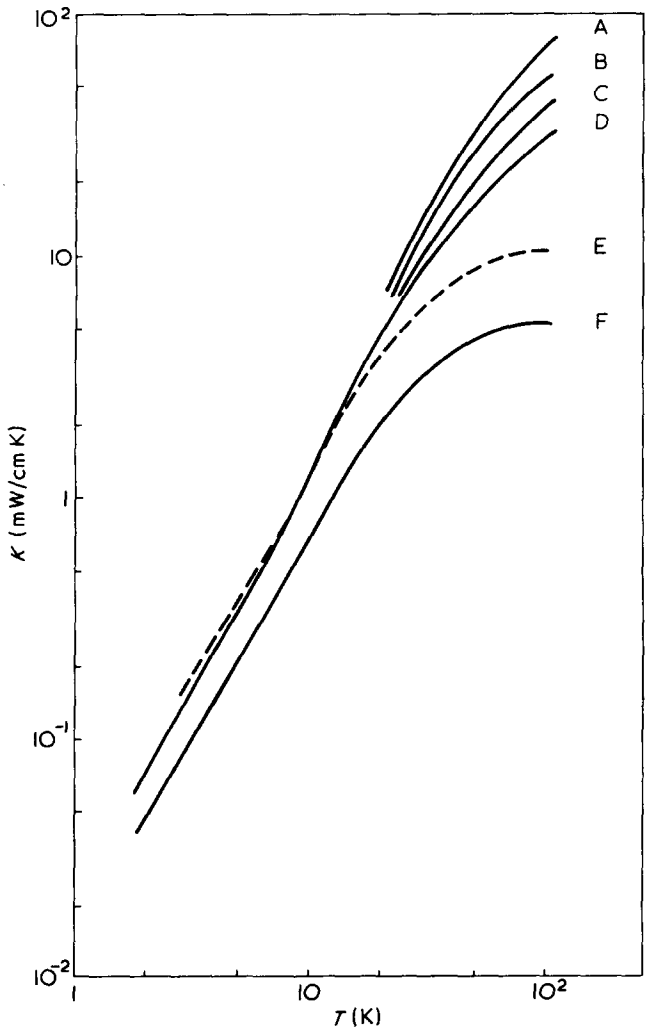

Figure 21 Thermal conductivity of extruded PE. The starting material is Rigidex 50 ($X \simeq 0.8$). $K_{/\!/}$: A, $\lambda = 20$: B, $\lambda = 13$; C, $\lambda = 9$, D, $\lambda = 5.4$; E, isotropic sample; F, $K_\perp$ ($\lambda = 5.4$). $K_\perp$ for other samples of $\lambda > 5.4$ follow the same curve as F. Data from ref 34

$$\frac{1}{K_\perp} = \frac{1}{2}\left[\left(\frac{1}{K_{/\!/}^u} + \frac{1}{K_\perp^u}\right) - \left(\frac{1}{K_{/\!/}^u} - \frac{1}{K_\perp^u}\right)\langle\cos^2\theta\rangle\right] \quad (18a)$$

$$\frac{1}{K_{/\!/}} = \left(\frac{1}{K_{/\!/}^u} - \frac{1}{K_\perp^u}\right)\langle\cos^2\theta\rangle + \frac{1}{K_\perp^u} \quad (18b)$$

where $K_{/\!/}^u$ and $K_\perp^u$ are the thermal conductivities of the basic unit along and perpendicular to the symmetry axis, θ is the angle between the symmetry axis and the draw direction and $\langle\cos^2\theta\rangle$ is the average of $\cos^2\theta$ for the aggregate. Since $\langle\cos^2\theta\rangle$ is equal to 1/3 for the isotropic state it follows from equation (18) that:

$$\frac{3}{K} = \frac{2}{K_\perp} + \frac{1}{K_{/\!/}} \quad (19a)$$

$$= \frac{2}{K_\perp^u} + \frac{1}{K_{/\!/}^u} \quad (19b)$$

where K is the thermal conductivity of the isotropic material.

With the aid of the pseudo-affine deformation scheme[31,67] $\langle\cos^2\theta\rangle$ was calculated as a function of draw ratio λ and equation (18) was found[31] to be in good agreement with the data for PVC. Since equation (19a) is independent of deformation scheme it in fact provides a better test for the model, and we are gratified to see that good agreement with data has indeed been obtained[30] for PVC, PMMA and PS. We note, however, that despite the success of the series model there is no *a priori* reason why the parallel model cannot be used. In general, one can only expect the two models to provide bounds for the actual values of the thermal conductivity[67,68].

Hansen and Ho[69] have also developed a model of the thermal conductivity of polymers which can account for the orientation effect. In analogy with the treatment employed for liquids a chain segment of a polymer is assumed to interact with its nearest neighbours at some frequency. Owing to the difference in magnitude of the intrachain and interchain forces the frequency of interaction for neighbours in the same chain is different from that for neighbours in different chains. With the further assumption that the energy transferred in each interaction is proportional to the energy difference between the interacting segments, they obtained the following expression:

$$\frac{K}{K_\perp} = \left(\frac{K_{/\!/}}{K}\right)^{1/2} \quad (20)$$

Although equations (19a) and (20) are very different in form it has been shown[1] that they do not predict very different numerical results within the bounds where experimental data are available.

Semicrystalline polymers

We have seen that the orientation effect on amorphous polymers is not very strong, which is at least partly due to the relatively low draw ratio attainable. However, the picture changes considerably for the semicrystalline polymers, the structure of which leads to very spectacular changes in both the magnitude and temperature dependence of the thermal conductivity for the highly oriented samples, as could be readily seen in *Figures 21* and *22*.

Before any attempt at an explanation of these results it is important to have an understanding of the morphological structure of these oriented polymers. It is now generally accepted[70,71] that when a semicrystalline polymer is drawn the spherulite is deformed and gradually broken up. Even at draw ratio as low as 4, wide-angle X-ray diffraction indicates quite a high degree of crystallite orientation with the chain axes aligned in the draw direction whereas low-angle X-ray diffraction gives either a four-point pattern or an arc with maximum intensity on the meridian. These results are consistent with a roof-top structure in which the lamellae are tilted at some angle to the draw direction while the chains in the lamellae are aligned in the draw direction. As the polymer is further deformed the tie molecules between the lamellae become highly extended and blocks of crystals are then pulled out. Finally, at a draw ratio of about 8, these blocks, which are still attached to each other by the tie molecules, become aligned along the draw axis giving rise to a fibrillar structure, and further drawing will only increase the number of taut tie molecules with the structure itself remaining unaltered. The above description is based largely on studies of PE but the main features are expected to be similar for other polymers[72,73]. The structure of hydrostatically extruded polymers is not well understood, but presu-

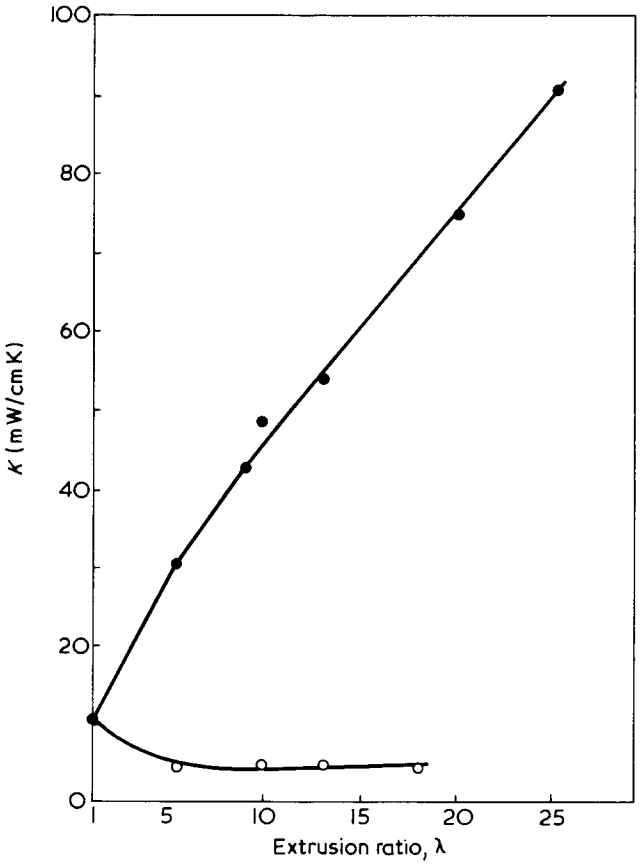

Figure 22 Thermal conductivity of PE at 100K as a function of extrusion ratio: ●, $K_{\parallel}$; ○, $K_{\perp}$. Data from ref 34

mably it is qualitatively similar to that of the drawn samples.

To continue our discussion of the thermal conductivity we see from *Figure 21* that below 10K $K_{\parallel} \simeq K_{iso} \simeq 1.5\, K_{\perp}$, that is, the anisotropy is very small. If we remember that this is the temperature range where the strong scattering mechanism arising either from thermal boundary resistance or correlation in sound velocity fluctuation is operative then the small anisotropy can probably be attributed to the relative insensitivity of this process to orientation.

Modified Maxwell model. The range above 30K is much more interesting since the thermal conductivity is strongly dependent on orientation. If we consider first the case of low draw ratios (say $\lambda < 5$) where the influence of the tie molecules is negligible then the only effect of drawing is to pull the chain axes of the crystallites towards the draw direction, this being characterized by the crystalline orientation function f_c given by:

$$f_c = \tfrac{1}{2}[3\langle\cos^2\theta\rangle - 1] \quad 0 \leqslant f_c \leqslant 1 \tag{21}$$

where θ is the angle between the chain axis and the draw direction and $\langle\,\rangle$ denotes the average over all crystallites. Wide-angle X-ray diffraction measurements[74–76] have shown that f_c for a number of polymers of widely different crystallinity (e.g. PVC, high and low density PE) have similar λ-dependence, that is, f_c increases very fast at low λ and reaches about 0.9 at $\lambda \simeq 4$. On the other hand, the amorphous orientation is rather low, with f_a less than 0.3 for $\lambda < 5$[77,78]. Therefore, if we take into consideration this result and the small orientation effect on amorphous polymers discussed previously it seems reasonable to describe the amorphous region by an isotropic conductivity K_a. Then using the modified Maxwell model the thermal conductivities $K_{\parallel}$ and $K_{\perp}$ can be calculated to be[62]:

$$\frac{K_{\perp} - K_a}{K_{\perp} + 2K_a} = X\left[\frac{k_{\perp} - 1}{k_{\perp} + 2} \times \frac{1 + \langle\cos^2\theta\rangle}{2} + \frac{k_{\parallel} - 1}{k_{\parallel} + 2} \times \frac{1}{2}\langle\sin^2\theta\rangle\right]$$

$$\simeq X\left[\frac{k_{\perp} - 1}{k_{\perp} + 2} \times \frac{1 + \langle\cos^2\theta\rangle}{2} + \frac{1}{2}\langle\sin^2\theta\rangle\right] \tag{22a}$$

$$\frac{K_{\parallel} - K_a}{K_{\parallel} + 2K_a} = X\left[\frac{k_{\parallel} - 1}{k_{\parallel} + 2} \times \langle\sin^2\theta\rangle + \frac{k_{\parallel} - 1}{k_{\parallel} + 2} \times \langle\cos^2\theta\rangle\right]$$

$$\simeq X\left[\frac{k_{\parallel} - 1}{k_{\parallel} + 2} \times \langle\sin^2\theta\rangle + \langle\cos^2\theta\rangle\right] \tag{22b}$$

where we have assumed that $k_{\parallel} = K_{c\parallel}/K_a \gg 1$. Since $\langle\cos^2\theta\rangle$ and $\langle\sin^2\theta\rangle$ can be calculated from f_c, and $k_{\perp}$ has already been determined from the data on isotropic materials (see *Figure 13*) there are no adjustable parameters in equation (22).

The predicted behaviour for PE and PP as a function of f_c is shown in *Figures 23* and *24*. It is clear that the model is in fair agreement with data and certainly gives the correct trends, namely: $K_{\parallel}$ increases rapidly with f_c while $K_{\perp}$ shows only a slight decrease. The observed $K_{\parallel}$ values for PE show a sudden sharp rise at $\lambda \gtrsim 4 (f_c \gtrsim 0.9)$, which indicates that effects other than crystalline orientation becomes important. This can be attributed to the increasing influence of the tie molecules and a different model has to be used in this range of high draw ratio. Since the tie molecules merely provide

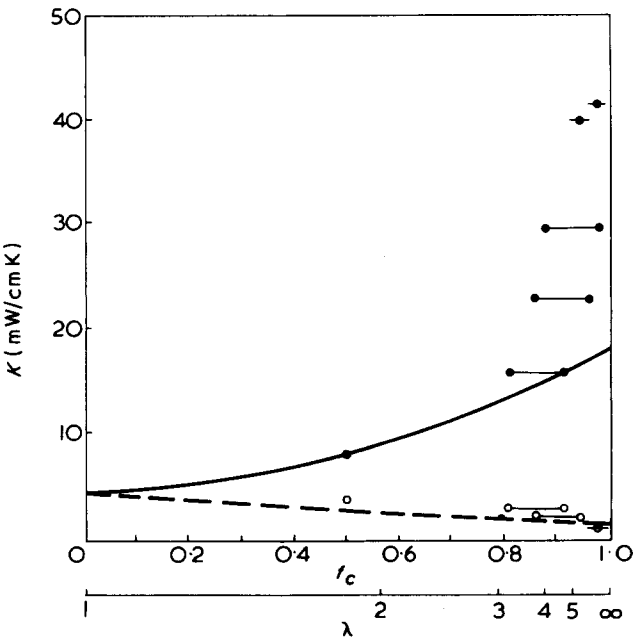

Figure 23 The thermal conductivity of oriented PE at 323K against the crystalline orientation function f_c. Data from ref 33. The horizontal error bar is due to the uncertainty in f_c since the measurements of the orientation function and thermal conductivity were made on different sets of samples. The theoretical curves $K_{\parallel}$ (——) and $K_{\perp}$ (– – –) are calculated from equation (22)

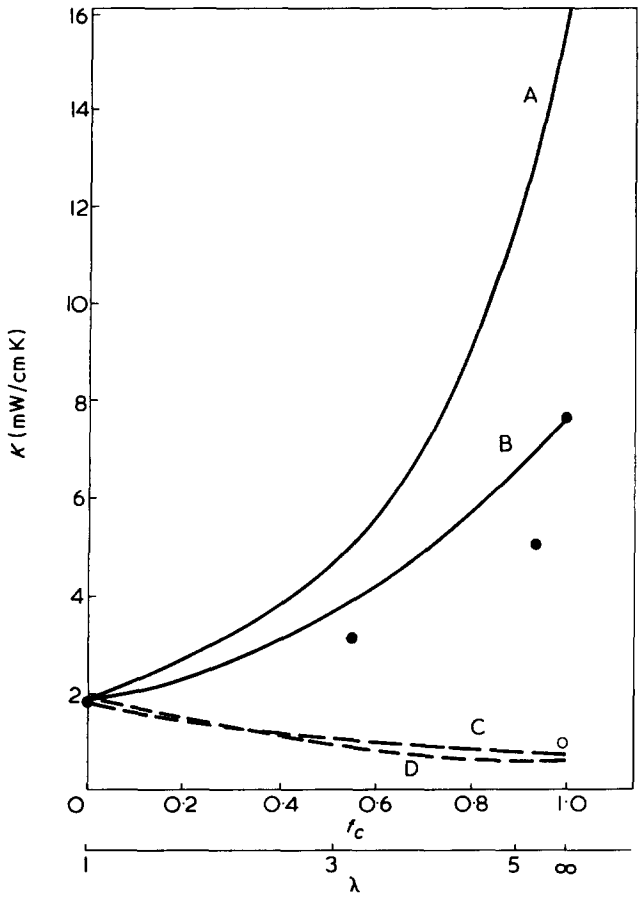

Figure 24 The thermal conductivity of extruded PP at 100K against the crystalline orientation function f_c. $K_{/\!/}$(●) and $K_\perp$ (○) data from ref 8. The theoretical curves for $K_{/\!/}$ (———) and $K_\perp$ (— — —) are calculated according to equation (22). $X = 0.79$ for the sample at $\lambda = 10.5$ while $X \simeq 0.62$ for the rest, so two sets of theoretical curves are given. A, $X = 0.79$; B, $X = 0.62$; C, $X = 0.62$; D, $X = 0.79$

paths of low thermal resistance between crystallites along the draw direction their effect on $K_\perp$ should be much smaller. This is consistent with the data in *Figure 23* which show that the present model gives a good descripton of $K_\perp$ even up to $\lambda = 10$. In addition, *Figure 24* shows that both $K_{/\!/}$ and $K_\perp$ for PP are not much affected by tie molecules even at $\lambda = 10.5$ and we can offer no explanation for this discrepancy at the moment.

For PE, the anisotropy $A = K_{/\!/}/K_\perp$ has also been measured as a function of λ for two samples of vastly different crystallinities ($X = 0.45$ and 0.74), the result clearly demonstrating the interplay between crystallinity and orientation (*Figure 25*). The most important feature, namely that the anisotropy A at any f_c is larger for higher crystallinity, is adequately reproduced by the model and quantitative agreement is satisfactory for $\lambda \lesssim 4$.

Since the above model is so successful in accounting for the λ-dependence at any temperature we expect it to be equally successful in predicting the temperature dependence of K, $K_{/\!/}$ and $K_\perp$. The temperature dependence of K of PE has already been discussed so we will now consider $K_{/\!/}$ and $K_\perp$.

It follows from equation (22b) that when $f_c = 1$ (perfect orientation) $K_{/\!/} = K_a(1 + 2X)/(1 - X)$, i.e. $K_{/\!/}$ is proportional to K_a and thus increases monotonically with temperature. However, we have seen that the thermal conductivity for isotropic PE ($f_c = 0$) decreases with rising temperature between 100 and 300K, so the model predicts that, as f_c increases from 0 to 1, the slope of the curve of $K_{/\!/}$ *versus* temperature will change gradually from negative to positive. Unfortunately, there are no data in this temperature range for checking this prediction. Nevertheless, the predicted monotonic increase of $K_{/\!/}$ with temperature is consistent with the data of extruded PE between 30 and 100K (see *Figures 16* and *21*). The predicted temperature dependence of $K_\perp$ is vastly different since equation (22a) implies that even at $f_c = 1$ $K_\perp$ depends on both K_a and $K_{c\perp}$. If we follow the same argument used for isotropic PE we see that $K_\perp$ will have similar temperature dependence as K, again in agreement with the data in *Figures 16* and *21*.

Takayanagi model. We have seen that $K_{/\!/}$ of PE above $\lambda = 5$ is strongly influenced by the presence of tie molecules. To find out more about this effect let us consider the series of extruded samples of high density PE (Rigidex 50, $X \simeq 0.8$) which goes up to extrusion ratio as high at 25 (*Figures 21* and *22*). It is clearly seen that, above 30K, $K_{/\!/}$ continues to increase with λ, up to the highest λ available. Similar increase in the axial Young's modulus $E_{/\!/}$ has also been found[34] and both these features can be explained by a series arrangement of amorphous and crystalline regions with intercrystalline bridges (taut tie molecules) connecting the crystallites[34]. The chains in the crystallites and the tie molecules are assumed to be aligned in the extrusion direction, which should be valid when $\lambda > 5$. Then the increase in $K_{/\!/}$ and $E_{/\!/}$ can be understood in terms of the increasing number of intercrystal-

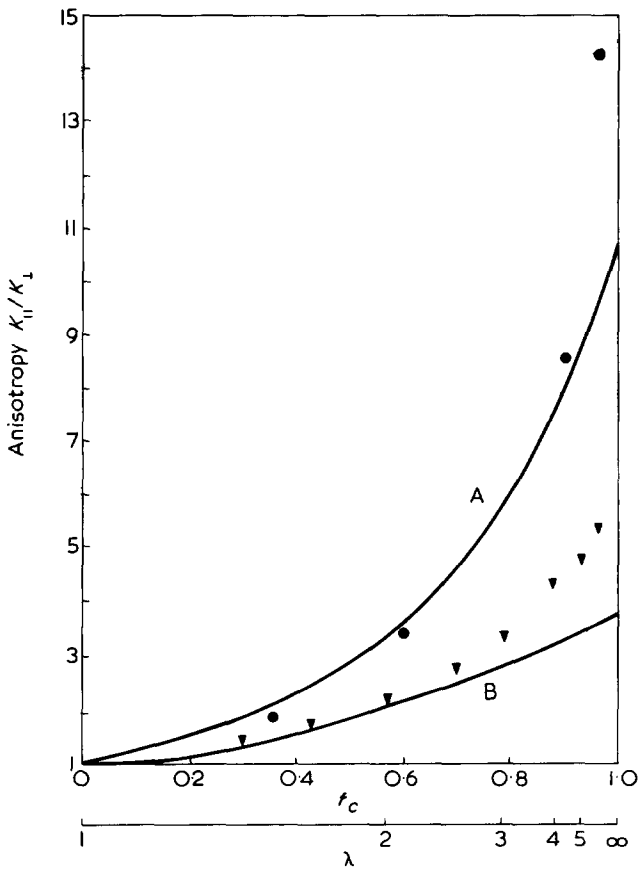

Figure 25 The anisotropy in the thermal conductivity of drawn PE at room temperature against the crystalline orientation function. ●, data ($X = 0.74$); ▼, data ($X = 0.45$) from ref 35. The theoretical curves are calculated according to equation (22). A, $X = 0.74$; B, $X = 0.45$

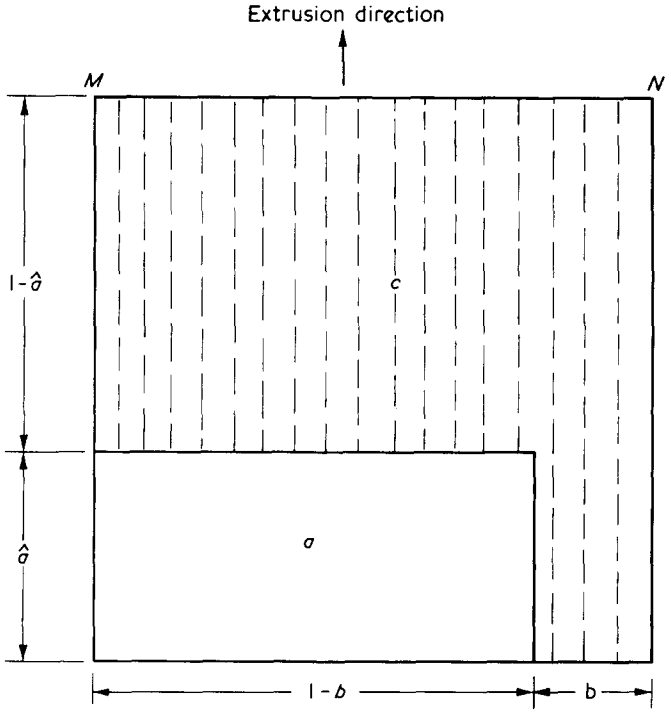

Figure 26 Schematic model of extruded PE showing the intercrystalline fraction, $\hat{a}$, containing the intercrystalline bridges b

line bridges with increasing λ. This kind of model has often been used in the analysis of the mechanical properties of oriented polymers (known in the mechanical case as the Takayanagi model[79]) and our modified version is shown schematically in *Figure 26*. If we assume that the intercrystalline bridges have the same thermal conductivity and modulus as the crystallites, then we can obtain the following expressions for $K_\parallel$ and $E_\parallel$:

$$\frac{1}{K_\parallel} = \frac{1-\hat{a}}{K_{c\parallel}} + \frac{\hat{a}}{bK_{c\parallel} + (1-b)K_a} \tag{23}$$

$$\frac{1}{E_\parallel} = \frac{1-\hat{a}}{E_{c\parallel}} + \frac{\hat{a}}{bE_{c\parallel} + (1-b)E_a} \tag{24}$$

where the subscripts a and c refer to the amorphous and crystalline phases, respectively.

In the temperature range above 30K $bK_{c\parallel} \gg (1-b)K_a$ if b is not too small (say >0.02), so equation (23) reduces to:

$$\frac{K_\parallel}{K_{c\parallel}} \simeq b[b(1-\hat{a}) + \hat{a}]^{-1} \tag{25}$$

Similarly, in the plateau region of modulus (≃200K), $bE_{c\parallel} \gg (1-b)E_a$ and an equivalent expression for $E_\parallel$ can also be obtained. Combining these two expressions gives:

$$\frac{K_\parallel(T)}{K_{c\parallel}(T)} \simeq \frac{E_\parallel(200\text{K})}{E_{c\parallel}} \tag{26}$$

Since $K_\parallel(T)/E_\parallel(200\text{K})$ is known experimentally (*Figure 27*) and as $E_{c\parallel} \simeq 240$ GN/m^2 [80,81], equation (26) can be used to obtain an estimate of $K_{c\parallel}(T)$. The result at 100K is 310 mW/cm K, which is about 200 times the value of K_a and this justifies the assumption of $K_{c\parallel} \gg K_a$ employed in earlier analysis. We note that in terms of the model the amorphous fraction is given by $1 - X = \hat{a}(1-b)$, which, together with equation (25), give the values of a and b. It was found[34] that b increases from 0.02 to 0.09 as λ increases from 5.4 to 25 while $\hat{a}$ remains almost unchanged at 0.25. This small value for b at λ = 5.4 justifies the neglect of the effect of tie molecules in our previous analysis of samples of lower draw ratio. We further note that the approximations used to obtain equation (25) and the equivalent expression for $E_\parallel$ are fairly well justified since they would lead to at most 25% error in the worst case, i.e. the sample with the lowest extrusion ratio. The fact that there is little deviation from linearity in *Figure 27* could be due to the respective errors in the approximations which led to equation (26) cancelling out.

The data of $K_\parallel$ also give us some information on the temperature dependence of $K_{c\parallel}$. It follows from equation (25) that $K_{c\parallel}$ is proportional to $K_\parallel$ which varies roughly linearly with temperature between 50 and 100K (*Figure 21*). If the above analysis is repeated for this temperature range then the $K_{c\parallel}$ values (which varies from 150 to 310 mW/cm K) obtained can be substituted into equation (2) to give a rough estimate of the phonon mean free path along the chain direction of the crystallites. However, in this one-dimensional situation, the factor 1/3 should be replaced by 1 since this factor is actually the average of the square of the cosine of the angle between the mean free path and the transport direction. Moreover, the heat capacity term $C(T)$ should include only the contribution of the acoustical vibrations along the chains while the sound velocity v is an appropriate average of the longitudinal and transverse velocities of these vibrations. Fortunately, in the temperature range under

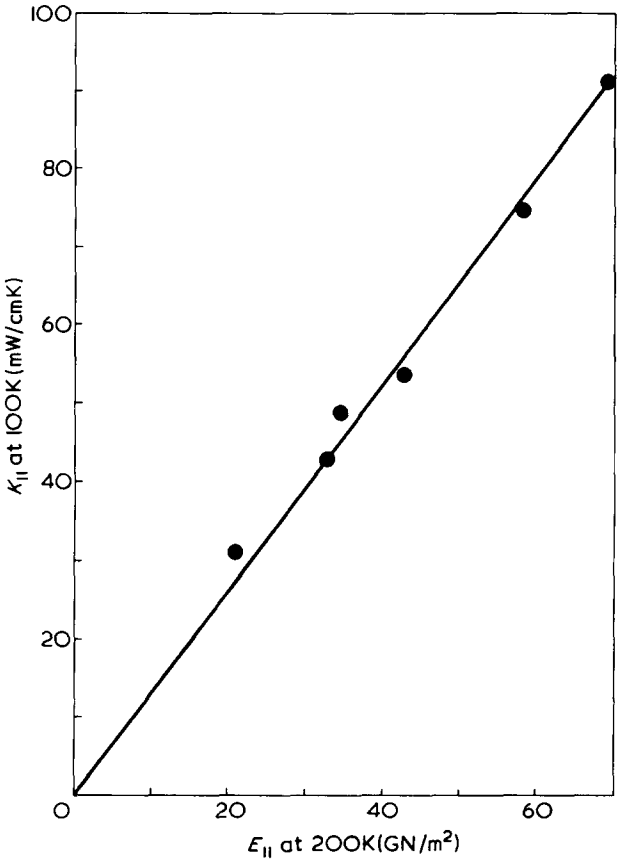

Figure 27 Variation of thermal conductivity along the extrusion direction at 100K with the Young's modulus in that direction measured at 200K

consideration, the observed heat capacity is contributed mostly by the acoustical vibrations along the chains[54] and can thus be used in our calculation. The longitudinal velocity is estimated from $v_L = (E_{c\parallel}/\rho_c)^{1/2} \simeq 15.5 \times 10^5$ cm/sec where $\rho_c = 1$ is the density of the crystallites. In addition, if we assume that the average force constant responsible for the transverse vibrations (C–C bending and twisting) is about 10 times smaller than that for the longitudinal vibrations (C–C stretching and bending) then $v_T \simeq (10)^{-1/2} v_L \simeq 4.9 \times 10^5$ cm/sec. Now if the average sound velocity is set roughly as $v = 3(1/v_L + 2/v_T)^{-1} \simeq 6.3 \times 10^5$ cm/sec we obtain $l_{c\parallel} = K_{c\parallel}/Cv \simeq$ constant $\simeq 75$ Å throughout the whole temperature range, which correlates roughly with (but is slightly smaller than) the dimension of the crystalline blocks in the extrusion direction[71]. Therefore we have to conclude that although tie molecules do provide paths of high thermal conductance along the extrusion direction there must also be severe phonon scattering at the junctions of crystalline blocks and tie molecules which gives rise to a temperature-independent effective mean free path. Considering the crudeness of the Takayanagi model and the limited temperature range over which data are available it seems rather premature to speculate on the physical reason for this behaviour. It is hoped that more data will be forthcoming so that we can find out whether such behaviour is observed over a wide temperature range.

Now if we consider the heat conduction perpendicular to the extrusion direction the situation is quite different. The above model gives:

$$K_\perp = K_{c\perp}(1-\hat{a}) + \frac{\hat{a}}{b/K_{c\perp} + (1-b)/K_a} \simeq (1-\hat{a})K_{c\perp} + \hat{a}K_a \qquad (27)$$

so that $K_\perp$ is roughly independent of λ, which is indeed the behaviour observed[34] (*Figure 22*). Taking $K_a = 1.8$ mW/cm K, we obtain $K_{c\perp} \simeq 6$ mW/cm K, in agreement with the value obtained previously from the modified Maxwell model (*Figure 13*). We have already seen that $K_{c\perp}$ has a different temperature dependence, varying roughly as T^{-1}. The mean free path in this direction is smaller than $l_{c\parallel}$ and is limited by Umklapp processes in our temperature range.

Aggregate model. The aggregate model, which is essentially a one-phase model, has also been applied to analyse the anisotropy of PE at room temperature[35]. It was emphasized that neighbouring crystalline lamellae have a definite orientation correlation and they form clusters within which the amorphous and crystalline regions are strongly coupled. These clusters can then be taken as the basic units of the aggregate and equations (18a) and (18b) can be combined to give:

$$A = \frac{1}{2}\left[\frac{2A^u + 1}{A^u - (A^u - 1)\langle\cos^2\theta\rangle} - 1\right] \qquad (28)$$

where $A^u = K^u_\parallel/K^u_\perp$ is the anisotropy of the basic unit. If we assume that the orientation of these units is adequately described by the crystalline orientation function f_c, then A can be calculated in terms of the adjustable parameter A^u. *Figure 28* shows the results for three samples of PE of different crystallinity and we can see that there is good agreement between theory and experiment. We note that the resulting value of the intrinsic anisotropy A^u varies from 7 for the sample at $X = 0.45$ to 26 at $X = 0.74$, i.e. A^u is crystallinity-dependent.

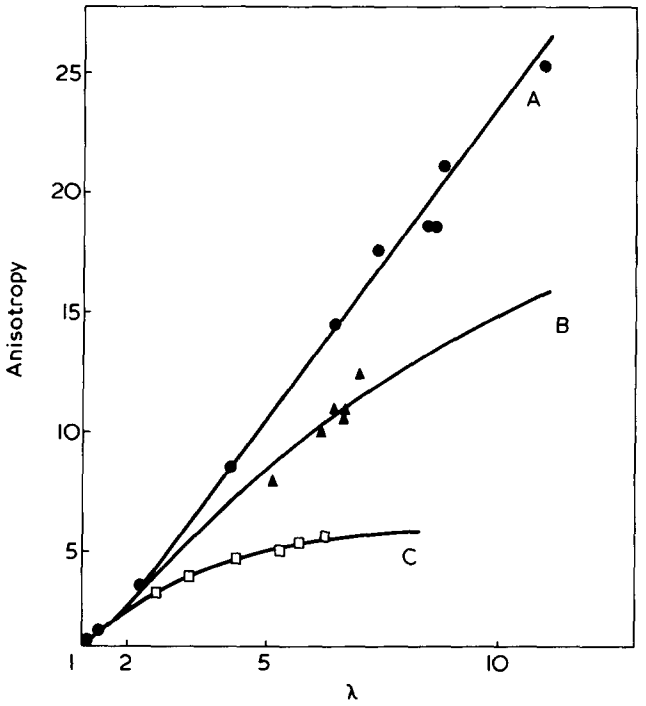

Figure 28 Variation of the anisotropy of PE with draw ratio. ●, $X = 0.74$; ▲, $X = 0.67$; □, $X = 0.45$. The theoretical curves are calculated according to equation (28) using $A^u = 26$, 16, 7, respectively, for the samples with $X = 0.74$, 0.67 and 0.45 (from ref 35)

The application of the aggregate model to the analysis of the moduli of semicrystalline polymers have received much greater attention[82,83] and the limitations of this model, which have been discussed in detail, apply equally to our case. In the following, we will give the main arguments and our own thoughts along the same lines. First, the assumption of unaltered basic units implies that there are no changes during the orientation process and this is certainly not true for crystalline polymers. Secondly, one would only expect the parallel and the series models to give the upper and lower bounds for the thermal conductivity of the aggregates, the correct value lying between these extremes. Therefore it is hard to justify the use of equation (28) (which is derived from the series model) to obtain a quantitative fit. Thirdly, since the orientation in the crystalline and amorphous regions differ by such a large extent (e.g. $f_c \simeq 0.9$ and $f_a < 0.3$ for PE at $\lambda = 4$) it is rather uncertain whether one should use f_c or an appropriate average of f_c and f_a to describe the orientation of the units. However, since equation (28) is able to predict the correct trend it seems that there is a definite correlation with f_c. Finally, in view of the large difference between $K_{c\parallel}$ and K_a, a two-phase model seems more appropriate and we have already shown that these data can be adequately described by the modified Maxwell model.

CONCLUSIONS

We have seen that, at low temperature, orientation has little effect on the thermal conductivity of semicrystalline polymers and this could probably be due to the relative insensitivity of the dominant phonon scattering mechanism (whether

arising from the correlation in the spatial fluctuation in sound velocity or acoustic mismatch at amorphous-crystalline interfaces) to orientation. In contrast, the thermal conductivity above 30K exhibits much larger anisotropy. At low draw ratio, this anisotropy is well described by the modified Maxwell model which takes into account the orientation of the chains in the crystallites. Since the chains are already aligned at $\lambda = 5$ further increase in $K_{\parallel}$ with λ can only be explained in terms of the increasing number of tie molecules, and the application of the Takayanagi model has put this analysis on a more quantitative basis. The aggregate model also seems to give encouraging results but we have seen that there are a few limitations. More work should be done to determine the conditions for the applicability of this model.

It is unfortunate that investigations of the thermal conductivity have been confined mainly to polyethylene and only within limited draw ratio and temperature ranges (either at room temperature or below 100K), so that some aspects of these models have not been adequately tested. For example, we have mentioned that the modified Maxwell model predicts a change of temperature dependence of $K_{\parallel}$ of polyethylene with orientation and this can easily be checked by measurements on samples with λ between 1 and 5. Moreover, measurements on highly drawn or extruded polyethylene should be extended to room temperature since it may be of considerable technological importance to check our expectation that $K_{\parallel}$ and the anisotropy A could reach 180 mW/cm K and 60, respectively. This $K_{\parallel}$ value is close to the thermal conductivity of stainless steel and is thus exceptionally high for polymers. Finally, data on a large variety of polymers in the widest possible draw ratio and temperature ranges would be most valuable.

ACKNOWLEDGEMENTS

The author is grateful to Professor I. M. Ward and Dr D. Greig of the University of Leeds, and Dr F. C. Chen and Dr K. Young of the Chinese University of Hong Kong for their critical readings of this article and for giving valuable comments and suggestions. Thanks are also due to Dr H. G. Killian and Dr M. Pietralla for sending us a preprint of their article.

REFERENCES

1 For reviews of these studies see Knappe, W. *Adv. Polym. Sci.* 1971, 7, 477; Kline, D. E. and Hansen, D. 'Thermal Characterization Techniques', (Eds P. E. Slade and L. J. Jenkins), Marcel Dekker, 1970, New York, p 247
2 Eiermann, K. and Hellwege, *J. Polym. Sci.* 1962, **57**, 99
3 Eiermann, K. *Kunstoffe* 1965, **55**, 335
4 Eiermann, K. *Kolloid-Z.* 1965, **201**, 3
5 Burgess, S. and Greig, D. *J. Phys. (D)* 1974, **7**, 2051
6 Burgess, S. and Greig, D. *J. Phys. (C)* 1975, **8**, 1637
7 Choy, C. L. and Greig, D. *J. Phys. (C)* 1975, **8**, 3121
8 Choy, C. L. and Greig, D. *J. Phys. (C)* 1977, **10**, 169
9 Reese, W. *J. Macromol. Sci. (A)* 1969, **3**, 1257
10 Reese, W. *J. Appl. Phys.* 1966, **37**, 864; Reese, W. *J. Appl. Phys.* 1966, **37**, 3227
11 Choy, C. L., Salinger, G. L. and Chiang, Y. C. *J. Appl. Phys.* 1970, **41**, 597
12 Stephens, R. B., Cieloszyk, G. S. and Salinger, G. L. *Phys. Lett. (A)* 1972, **38**, 215
13 Cieloszyk, G. S., Cruz, M. T. and Salinger, G. L. *Cryogenics* 1973, **13**, 718
14 For reviews of the work on inorganic amorphous solids see Zeller, R. C. and Pohl, R. O. *Phys. Rev. (B)* 1971, **4**, 2029; Stephens, R. B. *Phys. Rev. (B)* 1973, **8**, 2896
15 Klemens, P. G. 'Non crystalline Solids' (Ed. V. C. Frechette), Wiley, New York, 1960, p 508; Klemens, P. G. 'Physics of Non-crystalline Solids', (Ed. J. A. Prins), North Holland, Amsterdam, 1965, p 162
16 Morgan, G. J. and Smith, D. *J. Phys. (C)* 1974, **7**, 649
17 Anderson, P. W., Halperin and Varma, C. M. *Phil. Mag.* 1972, **25**, 1
18 Phillips, W. A. *J. Low Temp. Phys.* 1972, **7**, 351
19 Dreyfus, B., Fernandes, N. C. and Maynard, R. *Phys. Lett.* 1968, **12**, 647
20 Anderson, A. C., Reese, W. and Wheatley, J. C. *Rev. Sci. Instrum.* 1963, **34**, 1386
21 Reese, W. and Tucker, J. E. *J. Chem. Phys.* 1965, **43**, 105
22 Kolouch, R. J. and Brown, R. G. *J. Appl. Phys.* 1968, **39**, 3999
23 Scott, T. A., de Bruin, J., Giles, M. M. and Terry, C. *J. Appl. Phys.* 1973, **44**, 1212
24 Assfalg, A. *J. Phys. Chem. Solids* 1975, **36**, 1389
25 Neeper, D. A. and Dillinger, J. R. *Phys. Rev.* 1964, **135**, 1028
26 Garret, K. W. and Rosenberg, H. M. *J. Phys. (D)* 1974, **7**, 1247
27 Schmidt, C. *Cryogenics* 1975, **15**, 17
28 Little, W. A. *Can. J. Phys.* 1959, **37**, 334
29 Eiermann, K. *Kolloid-Z* 1964, **199**, 125
30 Hellwege, K. H., Hennig, J. and Knappe, W. *Kolloid-Z* 1963, **188**, 121
31 Hennig, J. *J. Polym. Sci (C)* 1967, **16**, 2751
32 Müller, F. H. *J. Polym. Sci. (C)* 1967, **20**, 61
33 Hansen, D. and Bernier, G. A. *Polym. Sci. Eng.* 1972, **12**, 204
34 Gibson, A. G., Greig, D., Sahota, M., Ward, I. M. and Choy, C. L. *J. Polym. Sci. (Polym. Lett. Edn)* 1977, **15**, 183
35 Kilian, H. G. and Pietralla, M. *Polymer* submitted for publication
36 Novichyonok, L. N. *Prog. Heat Mass Transfer* 1973, **5**, 293
37 Klemens, P. G. *Solid State Phys.* 1958, **7**, 1
38 Kittel, C. *Phys. Rev.* 1949, **75**. 972
39 Klemens, P. G. *Proc. Roy. Soc. (A)* 1951, **208**, 108
40 Ziman, J. M. 'Electrons and Phonons', Oxford University Press, London, 1968, p 248
41 Knappe, W., Lohe, P. and Wutschig, R. *Angew. Makromol. Chem.* 1969, **7**, 181
42 Hunklinger, S., Arnold, W. and Stein, S. *Phys. Lett. (A)* 1973, **45**, 311
43 Arnold, W., Hunklinger, S., Stein, S. and Dransfeld, K. *J. Non-Cryst. Solids* 1974, **14**, 192
44 Piche, L., Maynard, R., Hunklinger, S. and Jäckle, J. *Phys. Rev. Lett.* 1974, **32**, 1428
45 White, G. K. *Phys. Rev. Lett.* 1975, **34**, 204
46 Flubacher, P., Leadbetter, A. J., Morrison, J. A. and Stoicheff, J. *Phys. Chem. Solids* 1959, **12**, 53
47 Antoniou, A. A. and Morrison, J. A. *J. Appl. Phys.* 1965, **36**, 1873
48 Leadbetter, A. J. *Physics Chem. Glasses* 1968, **9**, 1
49 Choy, C. L., Hunt, R. G. and Salinger, G. L. *J. Chem. Phys.* 1970, **52**, 3629
50 Choy, C. L., Huq, M. and Moody, D. E. *Phys. Lett. (A)* 1975, **54**, 375
51 Rosenstock, H. B. *J. Phys. Chem. Solids* 1962, **23**, 659
52 Zaitlin, M. P. and Anderson, A. C. *Phys. Rev. Lett.* 1974, **33**, 1158
53 Tarasov, V. V. *Zh. Fiz. Khim.* 1950, **24**, 111
54 Wunderlich, B. and Baur, H. *Adv. Polym. Sci.* 1970, **7**, 151
55 Geil, P. H. 'Polymer Single Crystals', Interscience, New York, 1963
56 Statton, W. D. *J. Polym. Sci. (C)* 1967, **18**, 33
57 Kavesh, S. and Schultz, J. M. *J. Polym. Sci. (A-2)* 1970, **8**, 243
58 Loboda-Čačković, J., Hosemann, R., Čačković, H., Ferrero, F. and Ferracini, E. *Polymer* 1976, **17**, 303
59 Yeh, G. S. Y., Hosemann, R., Loboda-Čačković, J. and Čačković, H. *Polymer* 1976, **17**, 309
60 Takayanagi, M. and Kajiyama, T. *J. Macromol. Sci. (B)* 1973, **8**, 1
61 Sheldon, R. P. and Lane, K. *Polymer* 1965, **6**, 205
62 Choy, C. L. and Young, K. *Polymer* 1977, **18**, 769
63 Eucken, A. and Schröder, E. *Ann. Phys.* 1939, **36**, 609
64 de Araujo, F. F. T. and Rosenberg, H. M. *J. Phys. (D)* 1976, **9**, 665
65 Chen, F. C., Choy, C. L. and Young, K. *J. Phys. (D)* 1977, **10**, 57
66 Juijn, J. A., Gisolf, J. H. and de Jong, W. A. *Kolloid-Z.* 1973, **251**, 456
67 Ward, I. M. 'Mechanical properties of polymers', Wiley, New York, 1971, pp 253–262
68 Kausch-Blecken von Schmeling, H. H. *Kolloid-Z.* 1970, **237**, 251
69 Hansen, D. and Ho, C. C. *J. Polym. Sci. (A)* 1965, **3**, 659

70 Peterlin, A. *J. Polym. Sci. (C)* 1966, **15**, 427; *J. Polym. Sci.(C)* 1967, **18**, 123
71 Peterlin, A. *Kolloid-Z.* 1969, **233**, 857
72 Peterlin, A. and Balta-Calleja, F. J. *J. Appl. Phys.* 1969, **40**, 4238
73 Samuels, R. J. 'Structured Polymer Properties', Wiley, New York, 1974
74 Gupta, V. B. and Ward, I. M. *J. Macromol. Sci. (B)* 1971, **5**, 857
75 Williams, T. *J. Mater. Sci.* 1973, **8**, 59
76 Pietralla, M. *Kolloid-Z.* 1976, **254**, 249
77 Stein, R. S. *J. Polym. Sci. (C)* 1966, **15**, 185
78 Glenz, W. and Peterlin, A. *J. Macromol. Sci. (B)* 1970, **4**, 473; *J. Polym. Sci. (A-2)* 1971, **9**, 1191
79 Takayanagi, M. *Mem. Fac. Eng. Kyushu Univ.* 1963, **23**, 41
80 Sakurada, I., Ito, T. and Nakamae, K. *J. Polym. Sci. (C)* 1966, **15**, 75
81 Frank, F. C. *Proc. Roy. Soc. (A)* 1970, **319**, 127
82 Hadley, D. W. and Ward, I. M. 'Structure and Properties of Oriented Polymers', (Ed. I. M. Ward), Applied Science, New York, 1975, pp 264–289
83 Hadley, D. W. *Ibid* pp. 290–325